

Vu (2)

# NAVAL POSTGRADUATE SCHOOL

## Monterey, California

AD-A243 558



DTIC  
ELECTE  
DEC 20 1991  
S C D

# THESIS

HEAT TRANSFER ENHANCEMENT DUE TO  
BUBBLE PUMPING IN FC-72 NEAR THE  
SATURATION TEMPERATURE

by

Ali Sükrü Eren  
MARCH 1991

Thesis Advisor:

M.D. Kelleher

Approved for public release: Distribution is unlimited

91-18416



SI 121 184

01-10-1991

Unclassified

SECURITY CLASSIFICATION OF THIS PAGE

REPORT DOCUMENTATION PAGE				Form Approved OMB No 0704-0188	
1a. REPORT SECURITY CLASSIFICATION Unclassified			1b. RESTRICTIVE MARKINGS		
2a. SECURITY CLASSIFICATION AUTHORITY			3. DISTRIBUTION/AVAILABILITY OF REPORT Approved for public release: Distribution is unlimited		
2b. DECLASSIFICATION/DOWNGRADING SCHEDULE					
4. PERFORMING ORGANIZATION REPORT NUMBER(S)			5. MONITORING ORGANIZATION REPORT NUMBER(S)		
6a. NAME OF PERFORMING ORGANIZATION Naval Postgraduate School		6b. OFFICE SYMBOL (If applicable) ME	7a. NAME OF MONITORING ORGANIZATION Naval Postgraduate School		
6c. ADDRESS (City, State and ZIP Code)  Monterey, CA 93943-5000			7b. ADDRESS (City, State, and ZIP Code)  Monterey, CA 93943-5000		
8a. NAME OF FUNDING/SPONSORING ORGANIZATION		8b. OFFICE SYMBOL (If applicable)	9. PROCUREMENT INSTRUMENT IDENTIFICATION NUMBER		
8c. ADDRESS (City, State, and ZIP Code)			10. SOURCE OF FUNDING NUMBER		
			PROGRAM ELEMENT NO.	PROJECT NO.	TASK NO.
11. TITLE (Include Security Classification)  HEAT TRANSFER ENHANCEMENT DUE TO BUBBLE PUMPING IN FC-72 NEAR THE SATURATION TEMPERATURE					
12. PERSONAL AUTHORS ALI SÜKRÜ EREN					
13a. TYPE OF REPORT Master's Thesis		13b. TIME COVERED FROM _____ TO _____	14. DATE OF REPORT (Year, Month, Day) MARCH 1991		15. PAGE COUNT 81
16. SUPPLEMENTARY NOTATION The views expressed are those of the author and do not reflect the official policy or position of the Department of Defense or the U.S. Government					
17. COSATI CODES			18. SUBJECT TERMS (Continue on reverse if necessary and identify by block numbers)		
FIELD	GROUP	SUB-GROUP	boiling cooling, vertical channel, triggering of horizontally parallel placed chromel wires		
19. ABSTRACT (Continue on reverse if necessary and identify by block numbers) The use of boiling heat transfer in the liquid immersion cooling of electronic components has always been hampered by the excessive superheat necessary to initiate nucleation in the fluorinated hydrocarbons used as dielectric cooling fluids. In an attempt to overcome some of these difficulties, an experimental study of the effects of nucleate pooling boiling, on the heat transfer from surface near the boiling surface was conducted. An experimental chamber was constructed which had a column of four horizontal wires spaced 2.5 cm vertically from each other. The lowest wire was progressively heated from the natural convection region through the nucleate boiling region. A study was made of the effects of the boiling wake from the lowest wire on heat transfer from the upper wires. Under certain conditions heat transfer enhancements of up to 30% were obtained.					
20. DISTRIBUTION/AVAILABILITY OF ABSTRACT <input checked="" type="checkbox"/> UNCLASSIFIED/UNLIMITED <input type="checkbox"/> SAME AS RPT <input type="checkbox"/> DTIC USERS			21. ABSTRACT SECURITY CLASSIFICATION unclassified		
22a. NAME OF RESPONSIBLE INDIVIDUAL M.D. Kelleher			22b. TELEPHONE (Include Area Code) (408) 646-2530		22c. OFFICE SYMBOL ME/Kk

Approved for public release: Distribution is unlimited

Heat Transfer Enhancement Due to Bubble Pumping  
in FC-72 Near the Saturation Temperature

by

Ali Sükrü Eren  
Lieutenant Junior Grade, Turkish Navy  
Turkish Naval Academy, 1984

Submitted in partial fulfillment of the  
requirements for the degree of

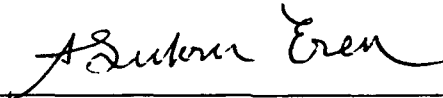
MASTER OF SCIENCE IN  
MECHANICAL ENGINEERING

from the

NAVAL POSTGRADUATE SCHOOL

MARCH 1991

Author:




Ali Sükrü Eren

Approved by:



M.D. Kelleher, Thesis Advisor



Anthony J. Healey, Chairman  
Department of Mechanical Engineering

## ABSTRACT

The use of boiling heat transfer in the liquid immersion cooling of electronic components has always been hampered by the excessive superheat necessary to initiate nucleation in the fluorinated hydrocarbons used as dielectric cooling fluids. In an attempt to overcome some of these difficulties, an experimental study of the effects of nucleate pooling boiling, on the heat transfer from surface near the boiling surface was conducted. An experimental chamber was constructed which had a column of four horizontal wires spaced 2.5 cm vertically from each other. The lowest wire was progressively heated from the natural convection region through the nucleate boiling region. A study was made of the effects of the boiling wake from the lowest wire on heat transfer from the upper wires. Under certain conditions heat transfer enhancements of up to 30% were obtained.

iii



Accession For	
NTIS GRA&I	<input checked="checked" type="checkbox"/>
DTIC Tab	<input type="checkbox"/>
Unannounced	<input type="checkbox"/>
Justification	
By	
Distribution/	
Availability Codes	
Dist	Avail and/or Special
A-1	

## TABLE OF CONTENTS

I.	INTRODUCTION . . . . .	1
	A. BACKGROUND . . . . .	1
	B. PREVIOUS WORK . . . . .	3
	C. OBJECTIVES . . . . .	7
II.	EXPERIMENTAL DESIGN . . . . .	8
	A. DESCRIPTION OF COMPONENTS . . . . .	8
	1. Test Chamber . . . . .	8
	2. Thermocouples . . . . .	9
	3. Heaters . . . . .	9
	4. Heat Exchangers . . . . .	10
	5. Aluminum Cover Plate . . . . .	10
	B. INSTRUMENTATION . . . . .	10
	1. Power to the Heaters . . . . .	11
	2. Temperature Measurement . . . . .	11
III.	EXPERIMENTAL PROCEDURE . . . . .	23
	A. NORMAL OPERATION . . . . .	23
	B. DATA REDUCTION . . . . .	24
IV.	RESULTS AND DISCUSSION . . . . .	27
	A. INDIVIDUALLY POWERED . . . . .	27
	B. PUMPING EFFECT . . . . .	29
V.	CONCLUSIONS . . . . .	50
VI.	RECOMMENDATIONS . . . . .	51
	APPENDIX A. SAMPLE CALCULATIONS . . . . .	52
	APPENDIX B. UNCERTAINTY ANALYSIS . . . . .	57
	APPENDIX C. CALIBRATION OF CHROMEL WIRES . . . . .	64
	APPENDIX D. SOFTWARE . . . . .	66
	LIST OF REFERENCES . . . . .	70
	INITIAL DISTRIBUTION LIST . . . . .	73

## LIST OF FIGURES

Figure 1.	System Configuration . . . . .	13
Figure 2.	Photograph of Test Apparatus. . . . .	14
Figure 3.	Isometric View of the Test Chamber. . . . .	15
Figure 4.	Cross Sectional View From the Top of the Test Section. . . . .	16
Figure 5.	Schematic Drawing of Test Section in Vessel. . . . .	17
Figure 6.	Voltage Determination for Thermoelectric Coolers. . . . .	18
Figure 7.	Technical Data for Thermoelectric Coolers. . . . .	19
Figure 8.	Cover Plate with Thermoelectric Coolers . . . . .	20
Figure 9.	Thermocouple Connection Schematic . . . . .	21
Figure 10.	The Locations of the Thermocouples in the Chamber. . . . .	22
Figure 11.	Wire Number 1 Individually Powered, Semi-log. . . . .	32
Figure 12.	Number 1 Heat Flux vs. Surface Temperature, Log-log. . . . .	33
Figure 13.	Number 3 Shows Less Overshoot. . . . .	34
Figure 14.	Number 1 at Different Times. . . . .	35
Figure 15.	All Wires Individually Powered. . . . .	36
Figure 16.	Best Fit Experimental Data Compared with Churchill (1975) Correlation. . . . .	37
Figure 17.	Subcooling. . . . .	38
Figure 18.	Pumping Effect with Wire Number 4 at 42,800 W/m <sup>2</sup> . . . . .	39
Figure 19.	Pumping Effect with Wire Number 4 (Detailed Figure). . . . .	40
Figure 20.	Wire Number 4 at Constant Heat Flux (38,600 W/m <sup>2</sup> ). . . . .	41
Figure 21.	Detail of Figure 20. . . . .	42

Figure 22.	Wire Number 3 at Constant Heat Flux Value of 37,490 W/m <sup>2</sup> . . . . .	43
Figure 23.	Wire Number 3 at 20,430 W/m <sup>2</sup> . . . . .	44
Figure 24a.	Wire Number 2 at 20,530 W/m <sup>2</sup> . . . . .	45
Figure 24b.	Detail of Figure 24a. . . . .	46
Figure 25a.	Wire Number 2 Kept at 212,700 W/m <sup>2</sup> . . . . .	47
Figure 25b.	Detail of Figure 25a. . . . .	48
Figure 26.	Wire Number 2 with Wire Number 3 at Constant Heat Flux. . . . .	49
Figure C1.	Chromel Wire Calibration. . . . .	65

## NOMENCLATURE

SYMBOL	UNITS	DESCRIPTION
A	m <sup>2</sup>	Area
$\beta$	1/K	Thermal Expansion Coefficient
C <sub>p</sub>	J/kg	Specific Heat
D	m	Diameter
g	m/sec <sup>2</sup>	Acceleration of gravity
G <sub>r</sub>	ND	Grashof Number
h	W/m <sup>2</sup> k	Heat Transfer Coefficient
k	W/mk	Thermal Conductivity
L	m	Heater Length
Q	W	Heat Transfer
q	W/m <sup>2</sup>	Heat Flux
Pr		Prandtl Number
$\Delta T_{\text{sat}}$		Wall Superheat, $T_w - T_{\text{sat}}$

## GREEK SYMBOLS

$\mu$	Ns/m <sup>2</sup>	Dynamic Viscosity
$\nu$	m <sup>2</sup> /s	Kinematic Viscosity
$\sigma$	N/m	Surface Tension
$\rho$	kg/m <sup>3</sup>	Density
$\omega$	various	Uncertainty in the Variables

## SUBSCRIPTS

l	Liquid
v	Vapor
sat	Saturation
sub	Subcooling



## **ACKNOWLEDGMENT**

The author would like to express his gratitude to Professors M.D. Kelleher and Y. Joshi for their advice, guidance and friendship in this endeavor.

He wishes to thank the members of the Mechanical Engineering Support Shop for their efforts, especially to Jim Schofield.

Many thanks are due to several other people and corporations without whose assistance this work could not have been completed.

## **I. INTRODUCTION**

### **A. BACKGROUND**

Research on pool boiling in electronic cooling systems has focused on three primary areas: (1) reducing the temperature excursion at incipient boiling, (2) reducing wall superheat during nucleate boiling and (3) enhancing critical heat flux (Mudawar, 1990). Since the heat transfer potential of nucleate boiling is well known, this regime was one natural selection for examination as a possible solution to this cooling problem. Nishikawa (1980) notes that there are two primary methods used to promote nucleate boiling. The first is to treat the surface in a manner that reduces its wettability. The second, more promising one, is to manufacture a surface with cavities which trap and hold vapor keeping the nucleation site active.

In recent years the drive toward higher heat flux and power density in electronic equipment has turned attention to the use of dielectric liquids. The 3M Corporation has commercially produced its "Flourinert" series of high dielectric, inert electronic cooling liquids. In contrast to water and other conventional coolants these liquids possess relatively low thermal conductivities and boiling points and small heats of vaporization. They demonstrate high wettability

on most surfaces. Their surface tensions are the lowest of any known liquids, resulting in near-zero wetting angles. This is significant because it eliminates many potential nucleation sites. High dielectric strength and high resistivity are some of the characteristics that make these liquids well suited for electronic applications. Especially, FC-72 is known as chemically stable and leaves no residue during boiling.

However, when using dielectric fluids, incipience superheat excursion is pronounced which leads to very high wall temperatures. A firm understanding of boiling incipience is required in order to implement effective cooling. Boiling can produce very large-scale heat transfer coefficients but it also introduces some problems: (i) Boiling restricts the physical design of the system. (ii) A high degree of superheat may be required if the surface is very smooth in order for nucleation to occur. Due to the high local heat flux the occurrence of periodic boiling may result in local turbulence, even damage of electronic components. (iii) Impurities concentration may result at the nucleation site.

Subcooling offers many advantages over saturated boiling for cooling large arrays of computer chips due to the decreased diameter and rapid collapse of departing bubbles.

In this study heat transfer enhancement due to bubble pumping in FC-72 was investigated. It is hoped that they will serve to identify some trends and provide a basis for further research on actual components and integrated circuits.

## B. PREVIOUS WORK

Hsu (1962) proposed a method for determining the range of active nucleation sites as a function of temperature or heat flux. This model revealed that the maximum and minimum sizes of active cavities are functions of subcooling, system pressure, physical properties and the thickness of the superheated liquid layer.

Bergles and Chu (1979) compared the nucleate pool boiling heat transfer characteristics of three copper Union Carbide High Flux test sections to a plain copper tube in distilled water and R-113. The experiments were conducted with three different treatments to the test surface prior to collecting data: subcooling; aging by preboiling in the pool; and heating the surface in air to remove all liquid in the pores. This research indicated:

1. Heat transfer coefficients for the porous surfaces were four to ten times higher than for the plain surfaces.
2. There was a significant temperature overshoot prior to the initiation of boiling and it was not very sensitive to aging or the power increment changes in water. These overshoots were sensitive to aging, initial subcooling and power increment changes in R-113.

Bergles et al. (1968), conducted nucleate pool boiling studies in water, R-113 and FC-78, using a 304 stainless steel tube. As heat fluxes were increased, the heat transfer coefficient followed the convective curve until a high

superheat was attained, and then a distinct increase in the heat transfer coefficient was noted as nucleation occurred. This was followed by an abrupt drop in all temperatures by as much as 27°F. It was also noted that the inception of nucleation could be triggered by vibrating the test surface. The conclusions drawn were:

The phenomenon of temperature overshoot hysteresis in ordinary liquids is due to two causes:

1. The existence of metastable bubbles which are triggered only at sufficiently high disturbance levels,
2. The deactivation of larger cavities by displacing the vapor by liquid during subcooling.

Many of the experimental reports published prior to 1986 are reviewed by Bar-Cohen and Simon (1988). They noted significant variations in the incipience superheat from one report to the next. The authors discussed possible mechanisms for delayed nucleation. Recently non-repeatable and unsteady behavior of boiling incipience for a highly-wetting dielectric liquid (R-113) was documented by You et al. (1989).

The bubble behavior from the nucleate boiling regime to the film boiling regime has not been clarified yet, except for liquid helium. The transient boiling experiment of liquid nitrogen at stepwise heat generation in a platinum wire was carried out by Kunito Okuyama (1989).

McAdams *et al.* (1949), reported the effect of dissolved air on forced-convection subcooled nucleate boiling of water where the dissolved air reduced the heat flux at boiling initiation.

Torikai *et al.* (1970), used platinum wires immersed in water to measure dissolved gas effect on the incipience wall superheat under reduced pressure conditions (0.05 - 1.0 Bar).

Surface enhancement is a very popular tool for improving pool boiling performance. Marto and Lepere (1982) found three commercially available enhanced boiling surfaces which shifted the boiling curve of FC-72 toward lower superheats compared to a plain copper surface. In a study by Berenson (1962), nucleate boiling heat transfer coefficients varied by 600% due to variation in surface finish. He emphasized the importance of the surface roughness. Recent investigations on surface effects in pool boiling by Chowdhury and Winterton (1985) show that heat transfer appears to be unaffected by contact angle.

The effects of flow velocity and subcooling on critical heat flux from a simulated electronic chip attached to the wall of a vertical rectangular channel was determined by Mudawar and Madox (1988). They concluded that heat flux was significantly enhanced by increasing the degree of subcooling.

The solubility of gas in highly-wetting dielectric fluids is of special concern. These fluids can contain up to 25 times more dissolved air by volume than can water: 48% air by volume

can be dissolved in FC-72 compared to 1.9% air by volume in water (3M Product Manual, 1987).

Experimental results presented by You, Simon and Cohen (1990) indicate that dissolved air plays an important role at incipience only when a very high dissolved air content is maintained. The surface tension value for FC-72 was estimated to have a 2% reduction due to high dissolved air content.

S.M. You *et al.* (1989) conducted an experiment in saturated R-113 fluid under atmospheric pressure with two types of wires. One is 0.13 mm diameter chromel wire (90% nickel) and the second is a thin platinum film on a quartz rod. They examined many pits of various sizes using a scanning electron microscope (SEM).

Bar-Cohen (1990) conducted experiments providing pool boiling characteristics for a number of commercially available inert liquids (FC-43, FC-72, FC-75, FC-77, FC-84, FC-87). Data were obtained with a classical 0.25 mm platinum wire heating element. He concluded that:

1. Nucleate boiling characteristics of these fluids depend on the heating surface,
2. Saturated pool boiling curves were almost identical with one another on a particular heater,
3. Superheat excursions at boiling incipience appear to always occur, but their extent can vary widely.

### **C. OBJECTIVES**

The objective of this work was to investigate the effects of the boiling wake from a heated wire on the heat transfer from wires placed within the wake. This work was carried out using the dielectric liquid FC-72.



## **II. EXPERIMENTAL DESIGN**

### **A. DESCRIPTION OF COMPONENTS**

Figure (1) shows the system configuration and identifies all major components. Figure (2) is a photograph of the apparatus.

The chamber consisted of a plexiglass box with an aluminum coverplate fitted with a rubber O-ring. This vessel has side wall heaters to allow the liquid to be preboiled for degassing before the run, and to maintain the liquid at saturation temperature throughout the run. The vapor was condensed and returned to the chamber by gravity from the aluminum cover plate condenser equipped with thermoelectric coolers. The following is a description of the test apparatus.

#### **1. Test Chamber**

The test chamber was constructed of plexi-glass of 1/2 inch thickness and had inside dimensions of 6 inches height, 6 inches length and 2 inches width. An isometric view of the chamber is presented in Figure (3). Side walls are glued to each other.

It has a 1 inch diameter hole and 1 inch protruding pipe and a copper elbow tube in the back face which is the pathway for the power and thermocouple wires. The chamber also allows the test section to slide in and out for the

experiment. Cross-sectional and schematic drawings of the test section in the chamber are presented in Figures (4) and (5) respectively. The chamber also contained two small (1/4 in) pressure equalization outlets, located at the top-right and the bottom-left of the front vertical surface. It is a simply a closed tank with an aluminum cover plate.

The test chamber is attached to a wood base in order to give better arrangement for cables and connections.

## **2. Thermocouples**

Thermocouples, 0.01 in (0.254 mm) in diameter, were used to take measurements. The thermocouples for the plate condensers (thermoelectric coolers which are located on top of the aluminum plate) were bonded in grooves by placing a small drop of Eastman 910 adhesive on the thermocouple bead. The two thermocouples then were placed in the designated line groove. Using a weight, pressure was applied until the adhesive set. After allowing for three hours cure time, the remainder of the groove was filled with Omega Bond 101 Epoxy and smoothed to the level of the aluminum plate inside face. The Omega Bond 101 Epoxy experienced little shrink after curing.

## **3. Heaters**

The side wall heaters were glued on either side walls of the chamber. The actual size of the heaters were 125 x 11 mm and they were subjected to 5 V, 2.5 amperes. The power load depended on the combination of the wires being heated.

#### **4. Heat Exchangers**

The three thermoelectric heat exchangers measure 1.56 x 1.56 inches and were placed on top of the aluminum cover plate. The power supply for these were determined by the related curves. The property curves and technical data are presented in Figures (6) and (7) respectively.

#### **5. Aluminum Cover Plate**

An aluminum plate of 1/2 inch thickness was used as a cover plate for the test chamber. The inside face of the plate had two thermocouple beads to monitor the condenser temperature. Three thermoelectric condensers were placed on top of the aluminum plate. A thin groove was cut around the edges of the inside face for a O-ring gasket. The plate was screwed over the test chamber with eight stainless steel screws of 1/16 inch diameter and compressed the O-ring to form a watertight seal. Figure (8) shows the cover from the top with the condensers on it.

#### **B. INSTRUMENTATION**

Separate voltage taps across the heating element and across the precision resistor are used to compute heater resistance and heating element power. The heating element temperature is computed from its resistance via temperature calibration curve obtained prior to the experiment.

## **1. Power to the Heaters**

Each heater was run in series with a precision resistor that was measured to have a 0.1 ohm resistance. All four heaters were in parallel with a Hewlett Packard model number 6289A, 0-40 volts, 0-1.5 amperes, DC power supply. Both the voltage across the precision resistor and the chromel wire were measured independently. The current to each heater was calculated by the product of the heater voltage and heater current. Both voltages were measured by a Hewlett Packard model 3852S data acquisition system containing a Hewlett Packard model 44701A digital voltmeter, all controlled by a Hewlett Packard model 300 computer.

## **2. Temperature Measurement**

The thermocouples for the bulk fluid, ambient, ice reference point and coolers inside plate temperatures were referenced individually to an electronic Ice Point Reference as seen in Figure (9). Each reference thermocouple was connected such that its constantan lead was connected to a constantan lead of the measurement thermocouple. The copper leads of each measurement and reference thermocouple were connected directly to a Hewlett Packard model 44705A 20 channel relay multiplexer and inserted into the data acquisition system. The data acquisition system then measures the ice referenced voltage of each thermocouple. The voltages were converted directly into temperatures in the controlling

computer program by using a fourth order polynomial, fit to the thermocouple manufacturer's calibration data for copper-constantan thermocouples (Hazard, 1986). The locations of the thermocouples in the chamber are presented in Figure (10).

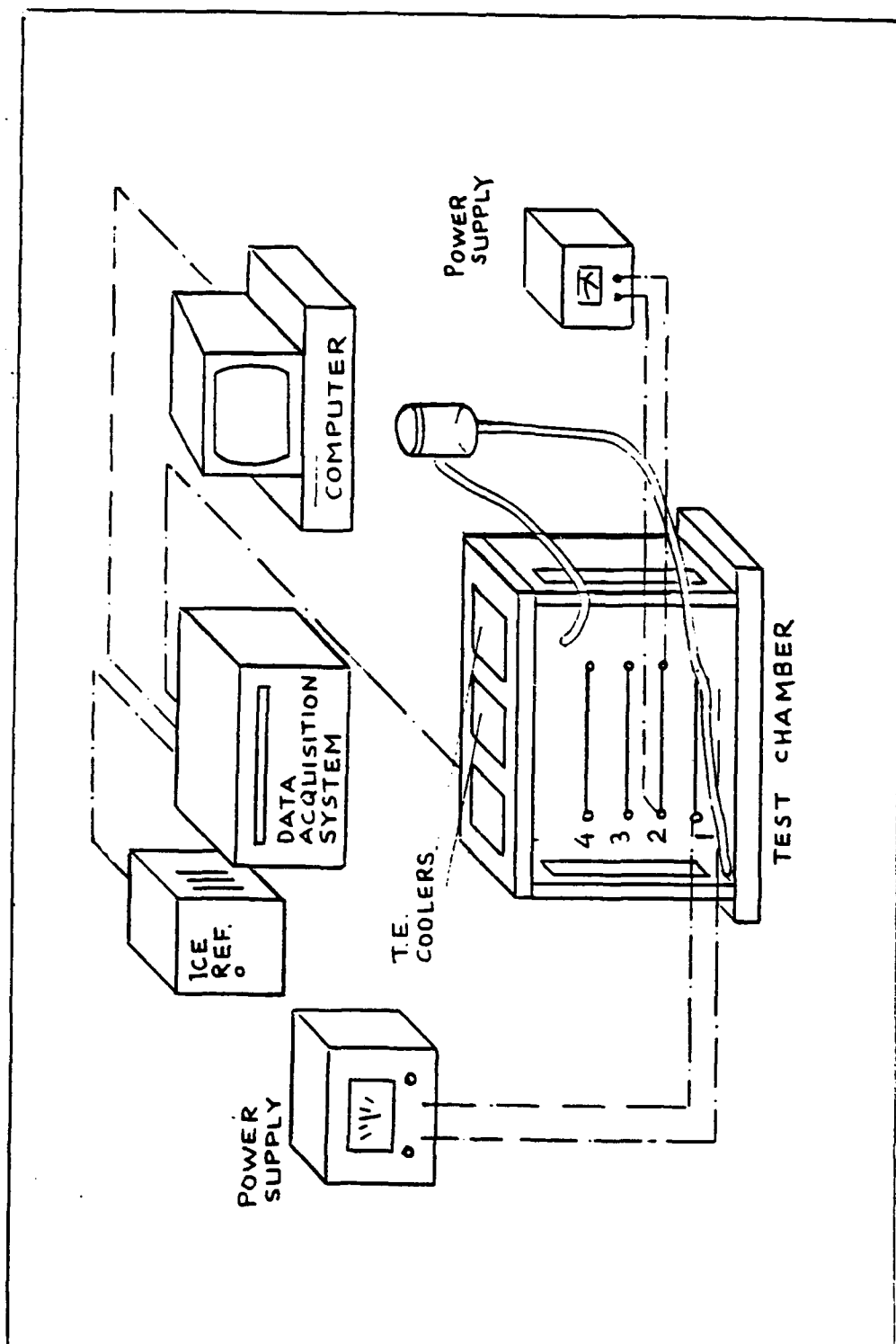
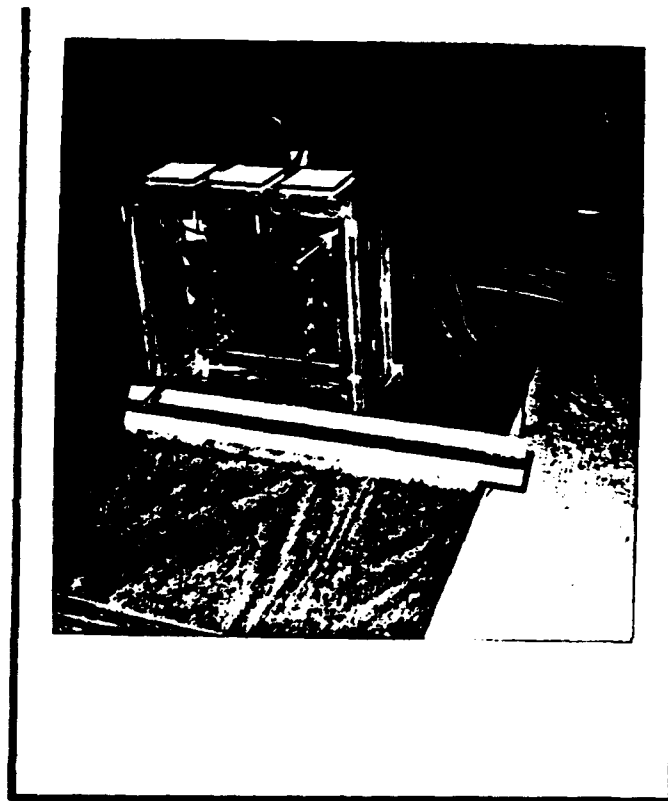
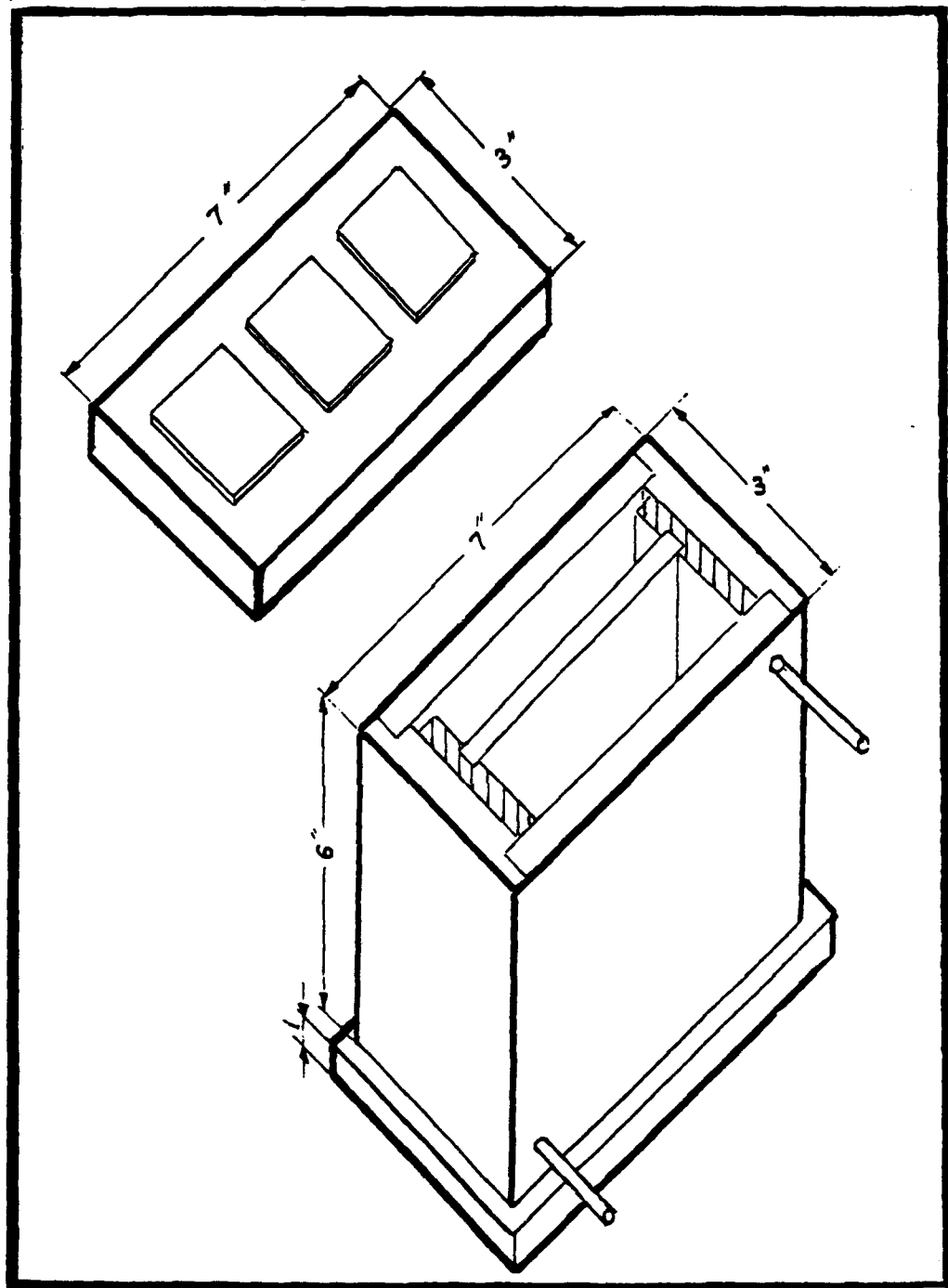


Figure 1. System Configuration.



**Figure 2. Photograph of Test Apparatus.**



**Figure 3. Isometric View of the Test Chamber.**



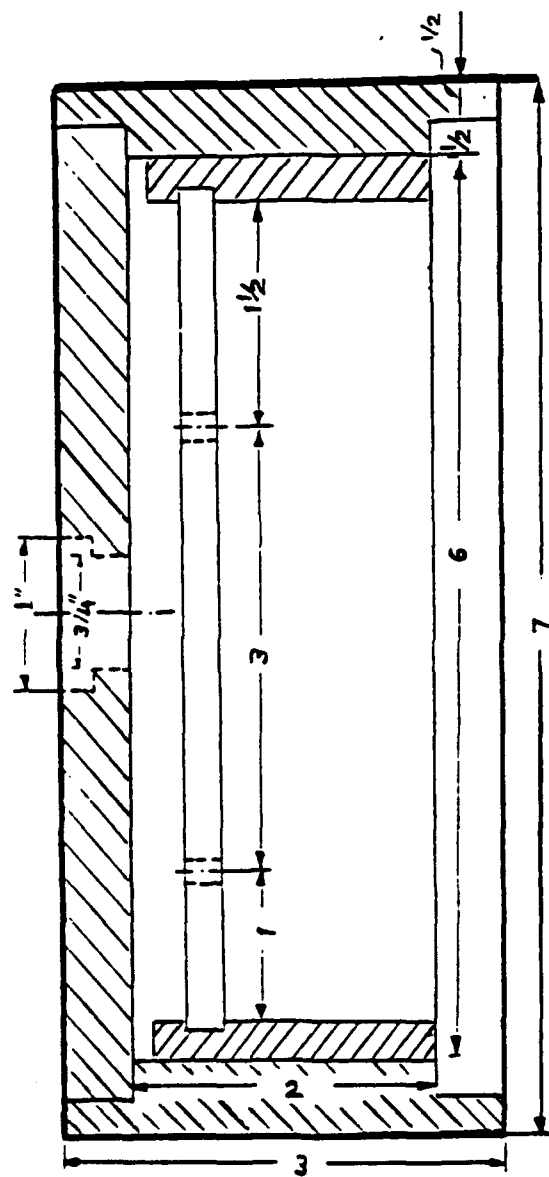
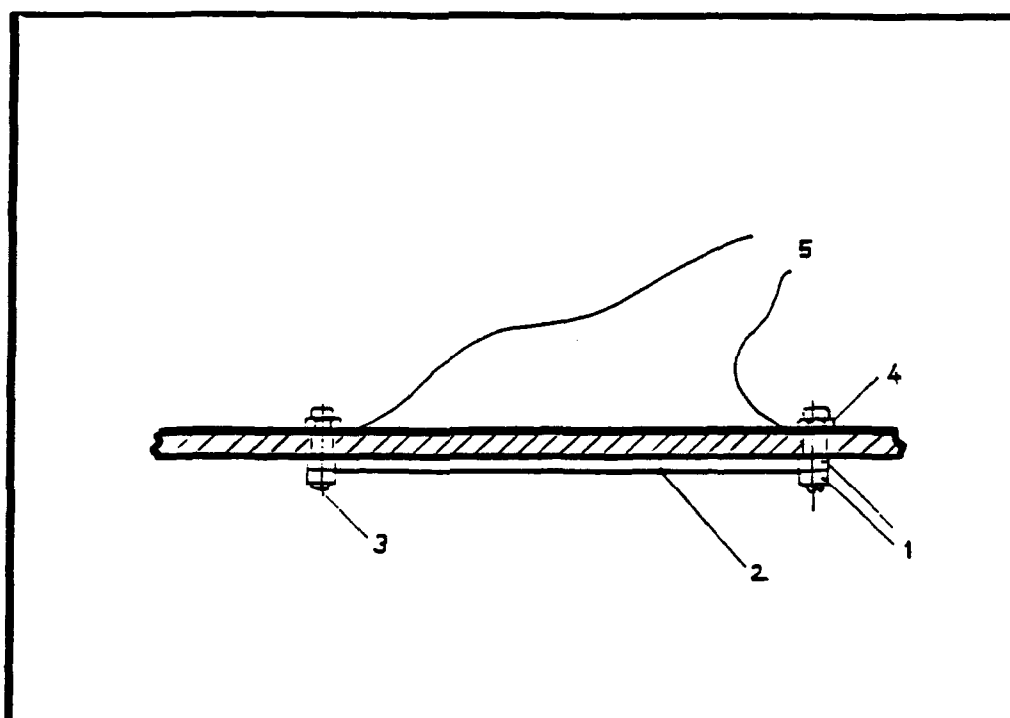


Figure 4. Cross Sectional View From the Top of the Test Section.



Key:

- 1. Washers
- 2. Chromel Wire
- 3. Screw
- 4. Nut
- 5. Power Line

**Figure 5. Schematic Drawing of Test Section in Vessel.**

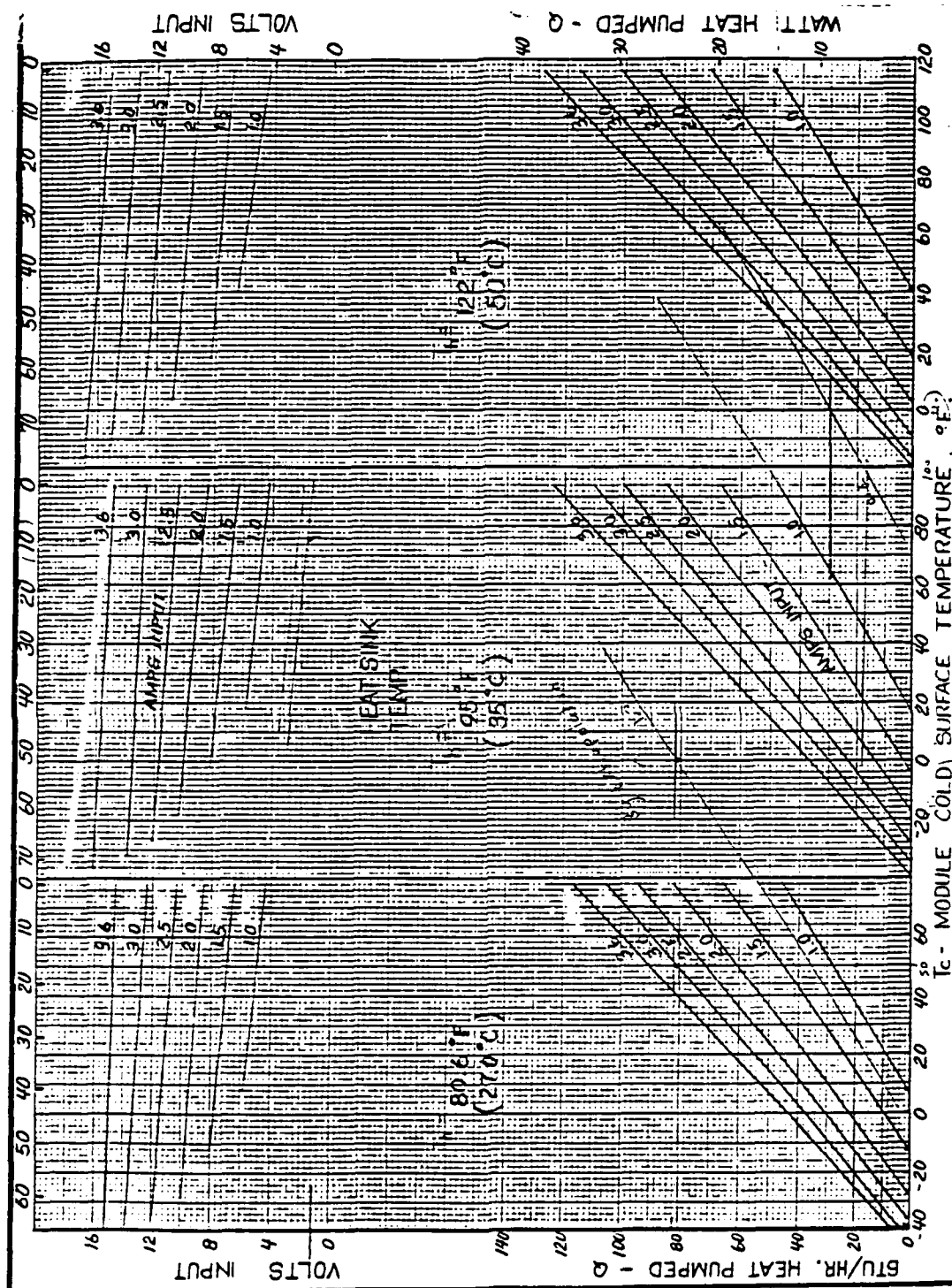


Figure 6. Voltage Determination for Thermoelectric Coolers.

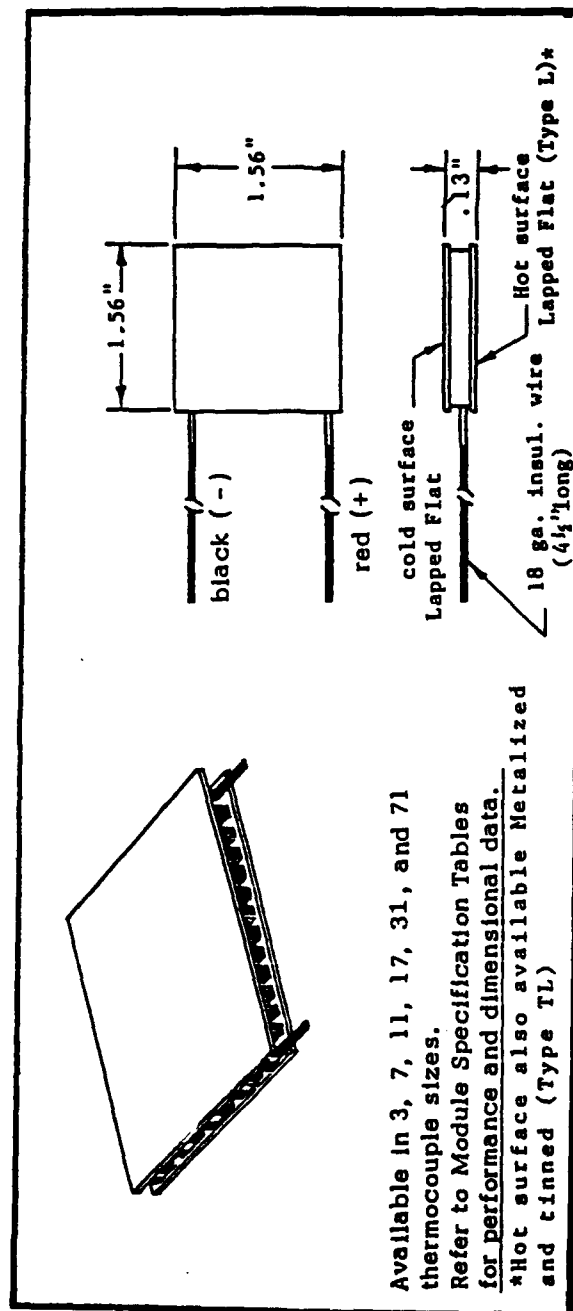


Figure 7. Technical Data for Thermoelectric Coolers.

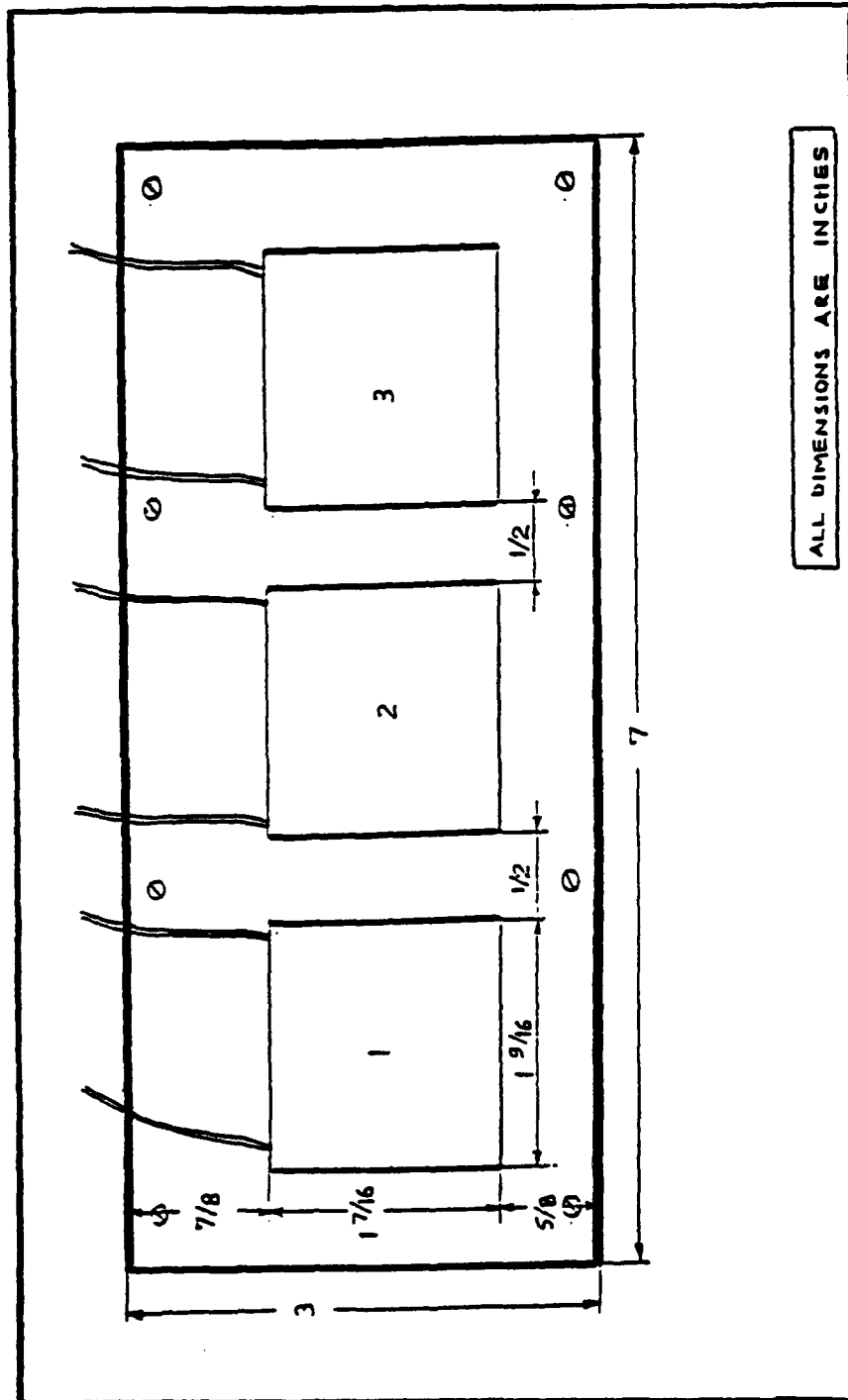
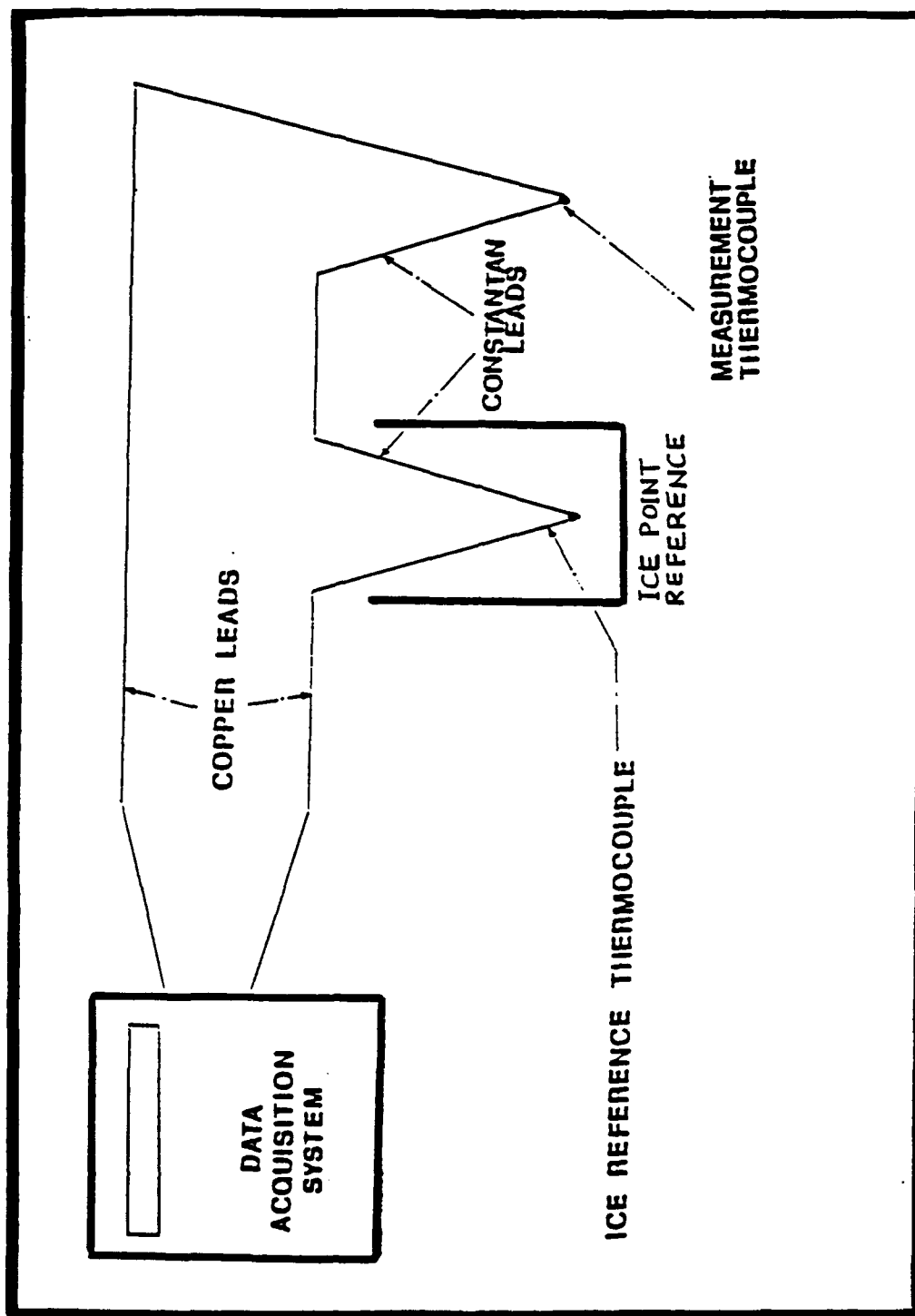
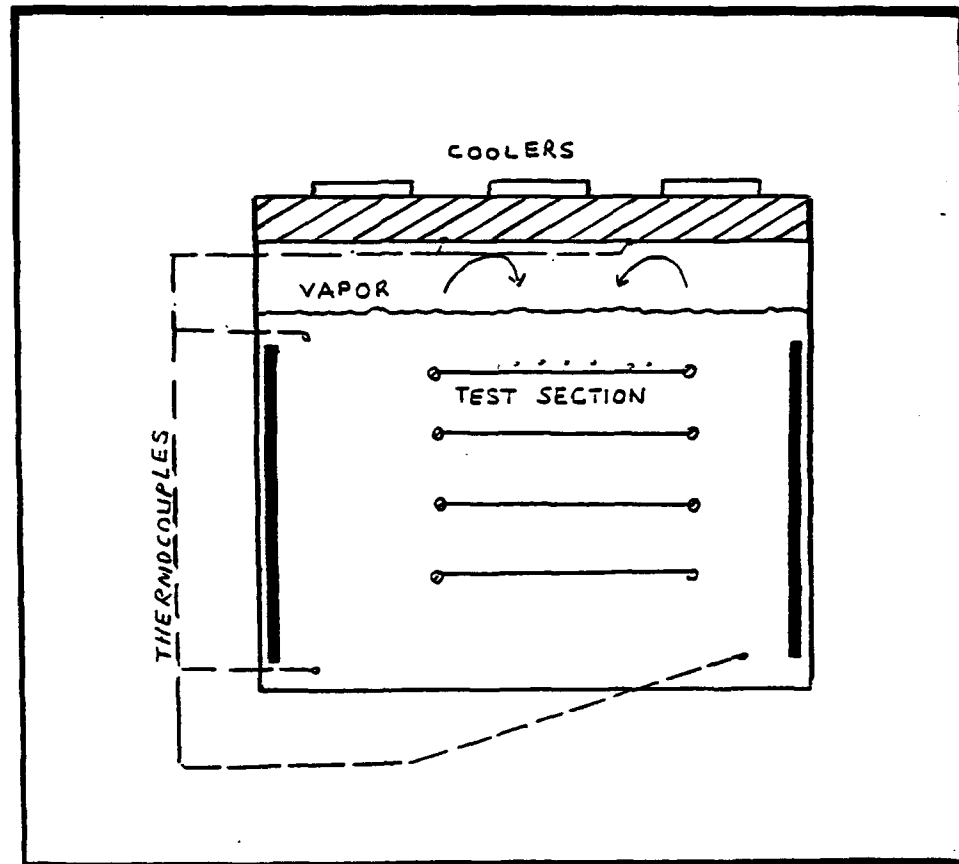


Figure 8. Cover Plate with Thermoelectric Coolers.



**Figure 9. Thermocouple Connection Schematic.**



**Figure 10. The Locations of the Thermocouples in the Chamber.**

### III. EXPERIMENTAL PROCEDURE

#### A. NORMAL OPERATION

In carrying out the experiments, the procedure was as follows:

1. The ice point reference device was turned on. A mercury thermometer inserted into the ice base ensured that the ice bath is at  $0 \pm 0.05^{\circ}\text{C}$  within one hour.

2. The data acquisition system was then turned on. The internal voltmeter in the data acquisition system requires one hour warm-up period.

3. The computer and printer were turned on. The data acquisition program contained in Appendix D was loaded.

4. The HP 6289A, 0-40 volt, DC voltage supply was set to zero and energized. The current limiter on the 40 volt power supply was set to the maximum current level.

A sampling of all thermocouple temperatures was performed and printed. The power was increased incrementally and the output from the power calculation program was checked.

The bulk fluid temperature as given by the wire resistance must match the value given by the bulk fluid thermocouples. When the results showed that the temperature stratification to be less than  $0.10^{\circ}\text{C}$  the experiment was ready to begin. The power to the test section is then increased by controlling the



test section heater voltage. The voltage was increased in 0.2 volt increments until the initiation of boiling occurred, at which time 0.1 volt increments were made until the maximum attainable heat flux was reached. This occurred at 5.7 volt for the power supply, making use of the HP 6289A, 0-40 volt, 0-1.5 Amperes DC voltage supply up to 8.1 volts, which corresponds to the maximum value. The power supply has a reset function to protect the device itself. The power is then decreased in the same fashion. At each power setting the system was permitted to stabilize for a few minutes and the following data were recorded: The heater voltage, precision resistor voltage, two thermocouple indications of thermoelectric cooler temperatures, and three thermocouple readings of pool temperatures. This procedure was repeated for every set up.

## **B. DATA REDUCTION**

The test wire temperature was found using the calibration formula between thermal resistance and temperature value of the chromel wire.

$$R = R_o (1 + \epsilon \Delta T)$$

where,

$$\Delta T = T_s - T_b$$

$T_s$  is the wall temperature

$T_b$  is the bulk liquid temperature

$\epsilon$  is the slope of the calibration curve.

Details of the calibration slope value are presented in Appendix C. This study utilizes the value of 0.0004 C/ohm offered by Kaye (1976).

The starting value of the wire resistance is accepted as the  $R_0$  in the previous formula.

The heat flux is calculated from the following formula:

$$Flux = Power/A$$

where,  $A = \pi D L$  is the total wetted surface area, and  $D$  and  $L$  are diameter and length of the wire respectively.

The bulk temperature of the liquid was measured by taking the arithmetic average of the three thermocouple readings.

$$T_{bulk} = (T_1 + T_2 + T_3) / 3$$

The Rayleigh number based on diameter is given as:

$$Ra_D = \frac{g \beta (T_s - T_b) D^3}{\nu \alpha}$$

where,

$$\epsilon = \frac{k_f}{(\rho_f C_p)}$$

All the properties in the above equations are calculated at the bulk temperature.

Determination of Nusselt number is:

$$\overline{Nu}_d = \frac{h D}{k}$$

where  $h$  is the heat transfer coefficient and was determined from

$$h = \frac{q''}{(T_s - T_{bulk})}$$

where,

$$\begin{aligned} T_s &= \text{wire surface temperature } (^{\circ}\text{C}) \\ h &= \text{heat transfer coefficient } (\text{W/m}^2 \cdot \text{C}) \\ q'' &= \text{heat flux } (\text{W/m}^2) \end{aligned}$$

Churchill and Chu (1975) have recommended a single correlation formula for the natural convection from long horizontal cylinders.

$$\bar{Nu}_d = \left\{ 0.60 + \frac{0.387 Ra_d^{1/6}}{[1 + (0.559/Pr)^{9/16}]^{8/27}} \right\}^2$$

It is valid for a wide Rayleigh number range

$$10^{-5} < Ra_d < 10^{12}$$

where the Prandtl number (Pr) is defined as

$$Pr = \frac{\nu}{\alpha}$$

#### **IV. RESULTS AND DISCUSSION**

Data were taken and the related graphs can be grouped for discussion purposes as:

1. individually powered wires
2. pumping effect runs

##### **A. INDIVIDUALLY POWERED**

Before investigating the pumping effect of the bubbles, individual boiling experiments on the wire heaters were conducted.

Figure (11) shows wire 1 (the lowest wire) where distinct single phase and nucleate boiling regimes are observed. When the heat flux was increased in small steps, the single phase curve reaches  $17^{\circ}\text{C}$  superheat. At about  $20^{\circ}\text{C}$  an abrupt temperature decrease occurs as nucleate boiling begins.

Figures (11) and (12) are essentially the same. The coordinates are heat flux versus surface temperature of the chromel wire. Figure (12) is on the log-log scale while Figure (11) is semilog graph.

Figure (13) is the single run boiling curve of heater number 3. It was the only one to show overshoot of less than  $7^{\circ}\text{C}$ .

Figure (14) for wire number 1 shows the same type of behavior as Figure (11). In this case data were taken at different times in order to demonstrate the repeatability of the experiments. Data points for two different runs did not coincide, but that is because the bulk fluid temperature is not the same for all experiments, but depends on the ambient temperature of the room.

Figure (15) indicates all individually powered heaters on the same graph. The difference in the overshoot may be because of the surface geometry of heater number 3.

The large aspect ratio of the heaters resulted in minimal conduction losses to the supports and yielded a uniform temperature along the length.

The boiling curves for all four wires are practically superimposable, even at the departure from nucleate boiling. They differ only in the heat flux at which boiling incipience occurred and at which full nucleate boiling began.

Figure (16) shows the best fit to the natural convection portion of the experimental data for wire number 1, and is compared with Churchill (1975) correlation values. There is a constant offset from the correlation values because of the wall effect except for the low Rayleigh numbers of that run which also shows considerable scatter in the data.

The saturation temperature of the FC-72 is about 56°C.  $T_{sat} - T_{bulk}$  is the subcooling. Figure (17) shows the effects of subcooling. At boiling incipience, a liquid mass near the

heated surface is slightly superheated, even though the bulk fluid is subcooled. Each run began with zero heating. The heat flux value was increased incrementally, continuing up the single-phase natural convection line until boiling was initiated. The figure indicates that as the subcooling increases the curve shifts to the left, displaying significant increases in the overshoot and heat fluxes. With bulk liquid at 15°C, it shows large amount of superheat, probably a bubble begins to form on the wire and as soon as the bubble grows a bit it encounters subcooled liquid and collapses. The liquid is so cold that it doesn't allow the bubble to grow. As the bulk temperature of the liquid gets warmer, it allows the bubbles to grow. Subcooling results in smaller bubbles, which are less likely to spread to neighboring nucleation sites than the larger bubbles associated with saturated boiling.

## **B. PUMPING EFFECT**

For this type of experiment, heater number 1 was used as the pumper.

Wire number 4 was fixed at various heat flux values, while heater number 1 was increased in a stepwise manner.

Figures (18) and (19) show the pumping effect of the bubbles generated by wire number 1 on the temperature of wire number 4. Clearly Figure (19) gives better understanding by way of marked corresponding points. As the temperature comes closer to the temperature at which the boiling incipience

starts, wire number 4 is little effected. Just after wire number 1 is subjected to overshoot it also has similar a experience, i.e., a sharp jump . Actually, it was the general pattern for most of the other runs. This suggests that boiling can be started by the pumping effects of the rising bubbles which trigger the heater located above it. The characteristics of the bubbles leaving the lower heater are uncertain. They may be the wake of the buoyancy-induced motion, especially when the upper wire was fixed at a high heat value. A similar trend can be observed from Figure (20). One thing to notice is that heater number 4 is fixed at a heat flux that corresponds to a starting value of surface temperature of 50°C for this run. This is below the temperature that meets the overshoot. Less jump in the temperature is associated with the lower fixed heat flux value. If we compare it with Figure (19), which was at higher heat value than this one, Figure (21) provides a detailed look at Figure (20).

Figure (22) shows wire number 3 fixed at 37,490 W/m<sup>2</sup>. It has the points marked in chronological order. The 3rd wire heater is located closer to the first wire than is the fourth wire, so it allows most of the bubbles to reach the upper heater with collapsing due to surrounding subcooled liquid FC-72.

Figure (23) shows another combination of heater number 3 with heater number 1. Heater number 3 is kept at 20,450 W/m<sup>2</sup>. This was very low heat flux value that the triggering effect

did not show itself. Bubbles still caused some decrease in the temperature of the upper wire.

Figures (24a) and (24b) show very similar results. In this case wire number 2 is kept at  $20,530 \text{ W/m}^2$ . Since wire number 3 is the closest to wire number 1. Being so close helped it to lose some heat corresponding to a decrease in its temperature.

Figures (25a) and (25b) show no effect from the bubbles from below. Here heater number 2 is kept at a very high heat flux of  $212,700 \text{ W/m}^2$ , which is already boiling. It is not sensitive any more to the bubbles produced by heater number 1. Consequently no jumps or apparent decrease on the surface temperature of the number 4 wire are seen.

Figure (26) shows similar trend as the early graphs. In this case the bubbles are produced by wire number 2 and the effects on wire number 3 are presented. Heater number 3 had the temperature decrease as the pumper had overshoot experience.



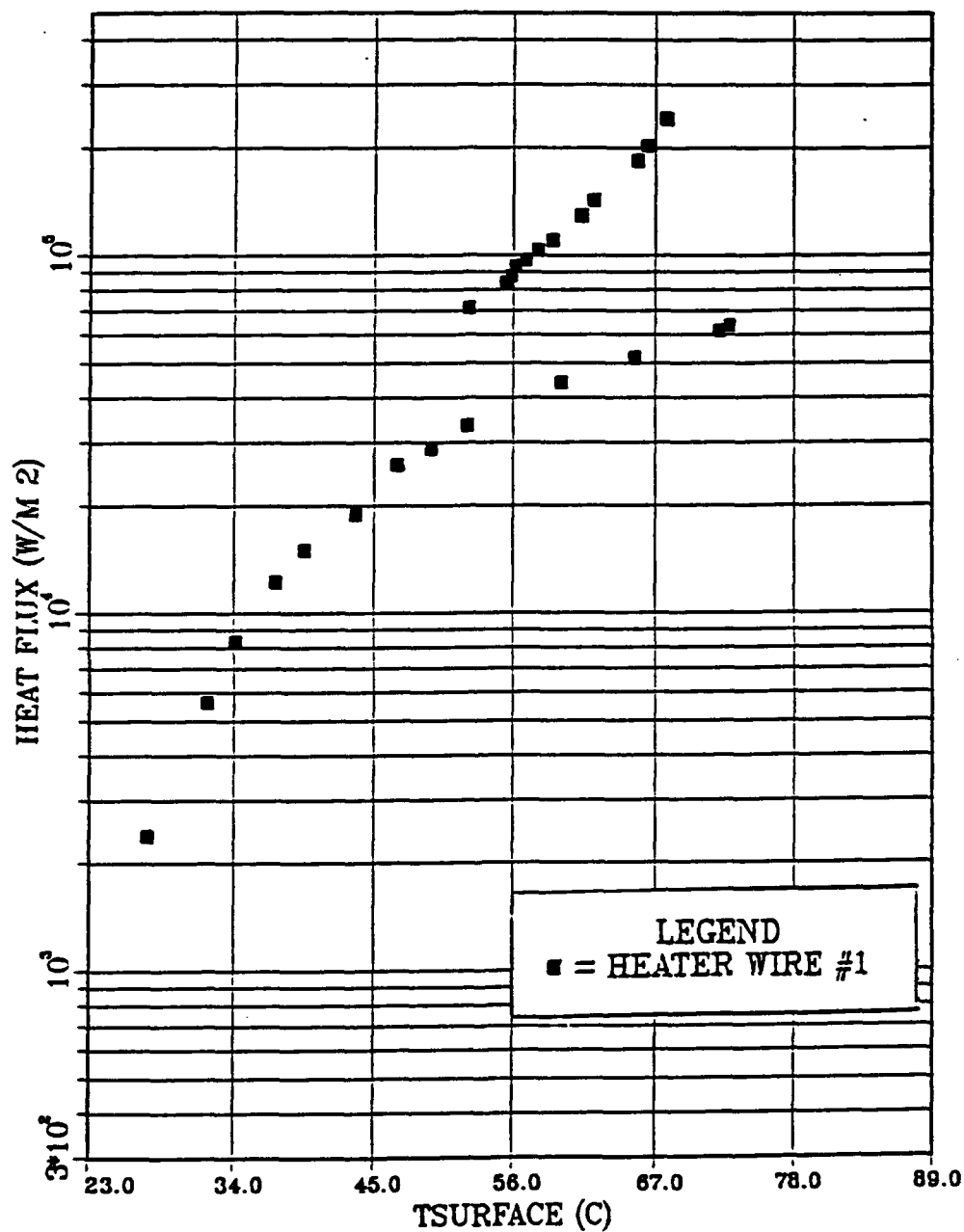


Figure 11. Wire Number 1 Individually Powered, Semi-log.

# INDIVIDUALLY POWERED

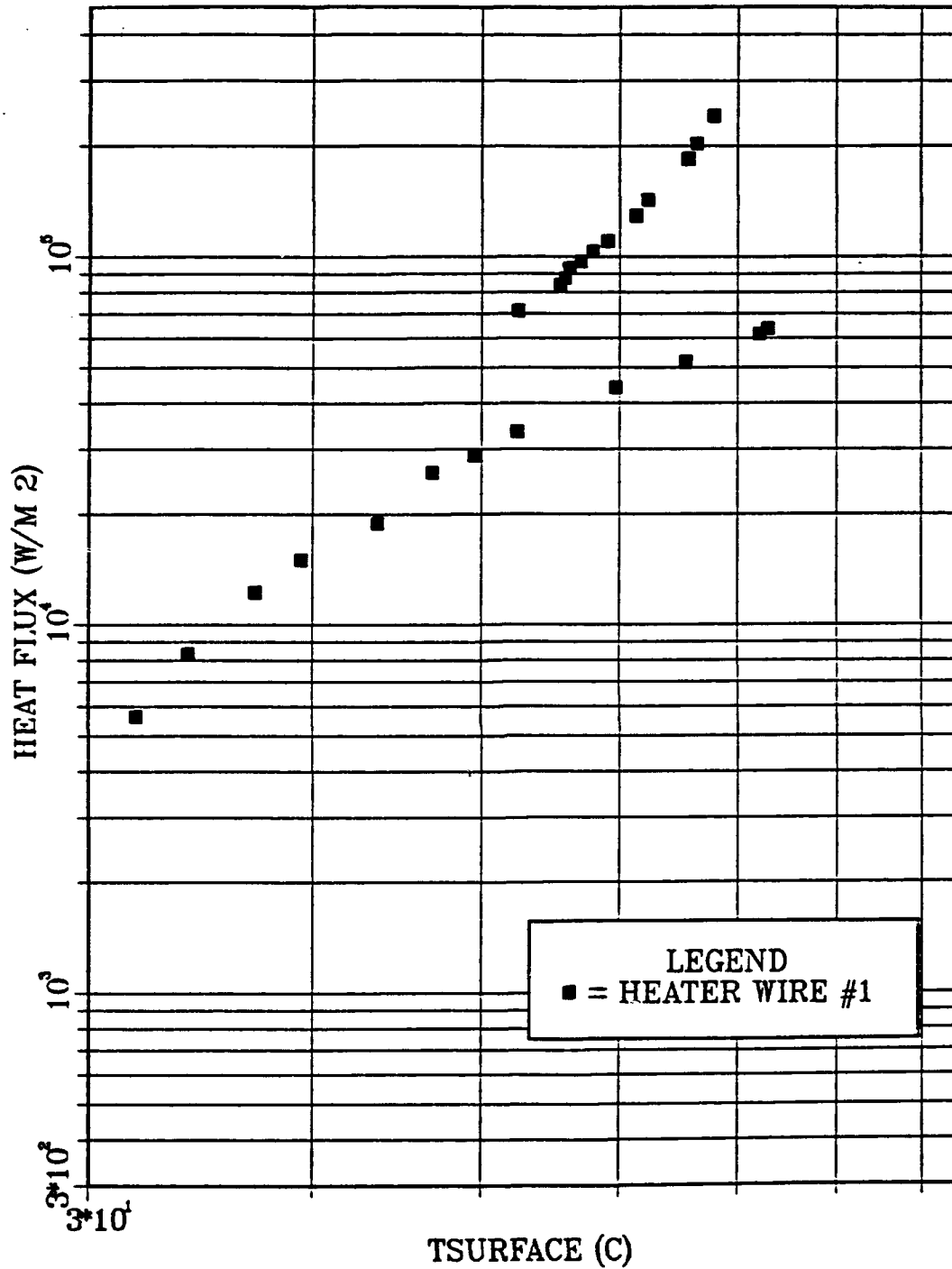


Figure 12. Number 1 Heat Flux vs. Surface Temperature, Log-log.

## INDIVIDUALLY POWERED

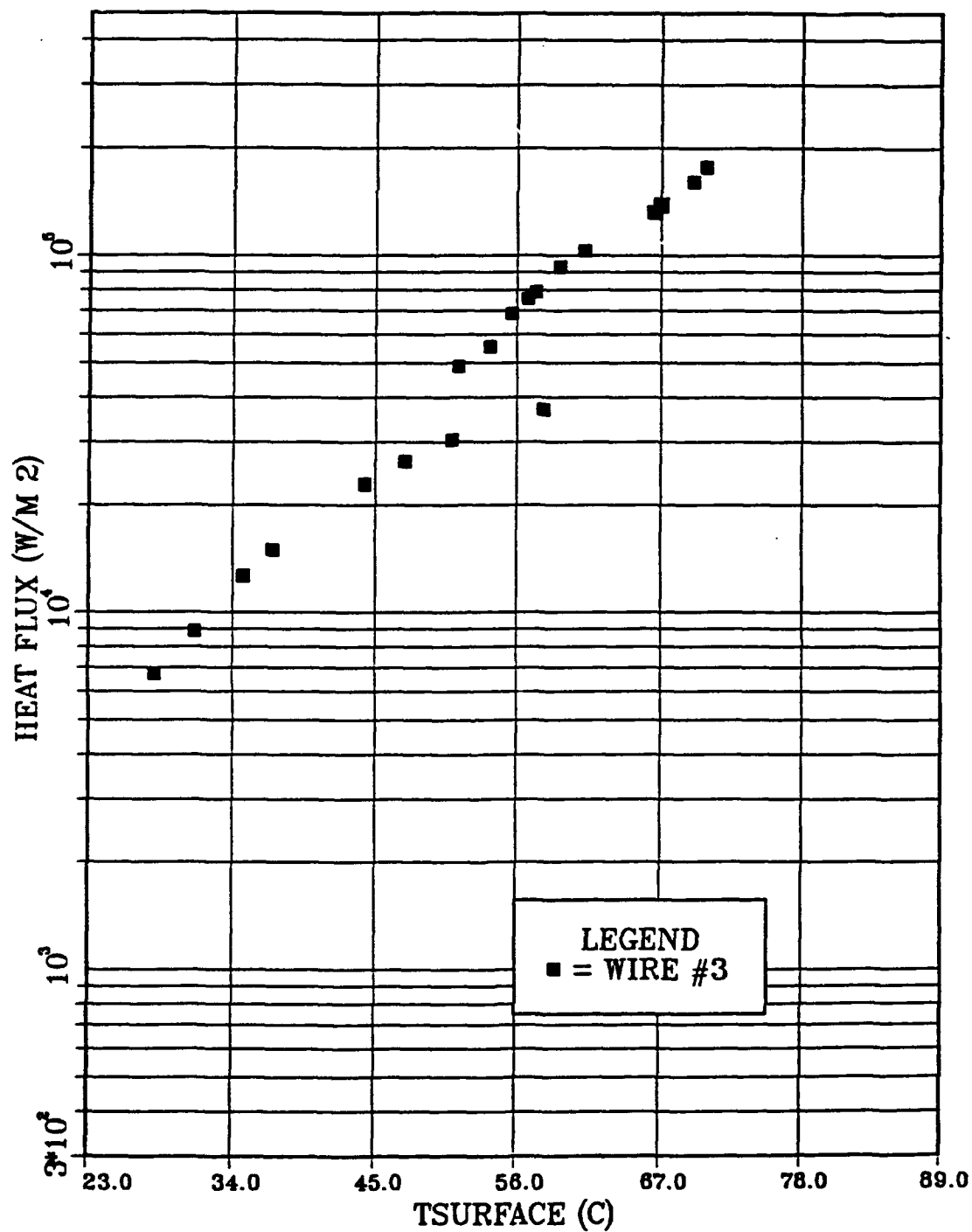


Figure 13. Number 3 Shows Less Overshoot.

# INDIVIDUALLY POWERED

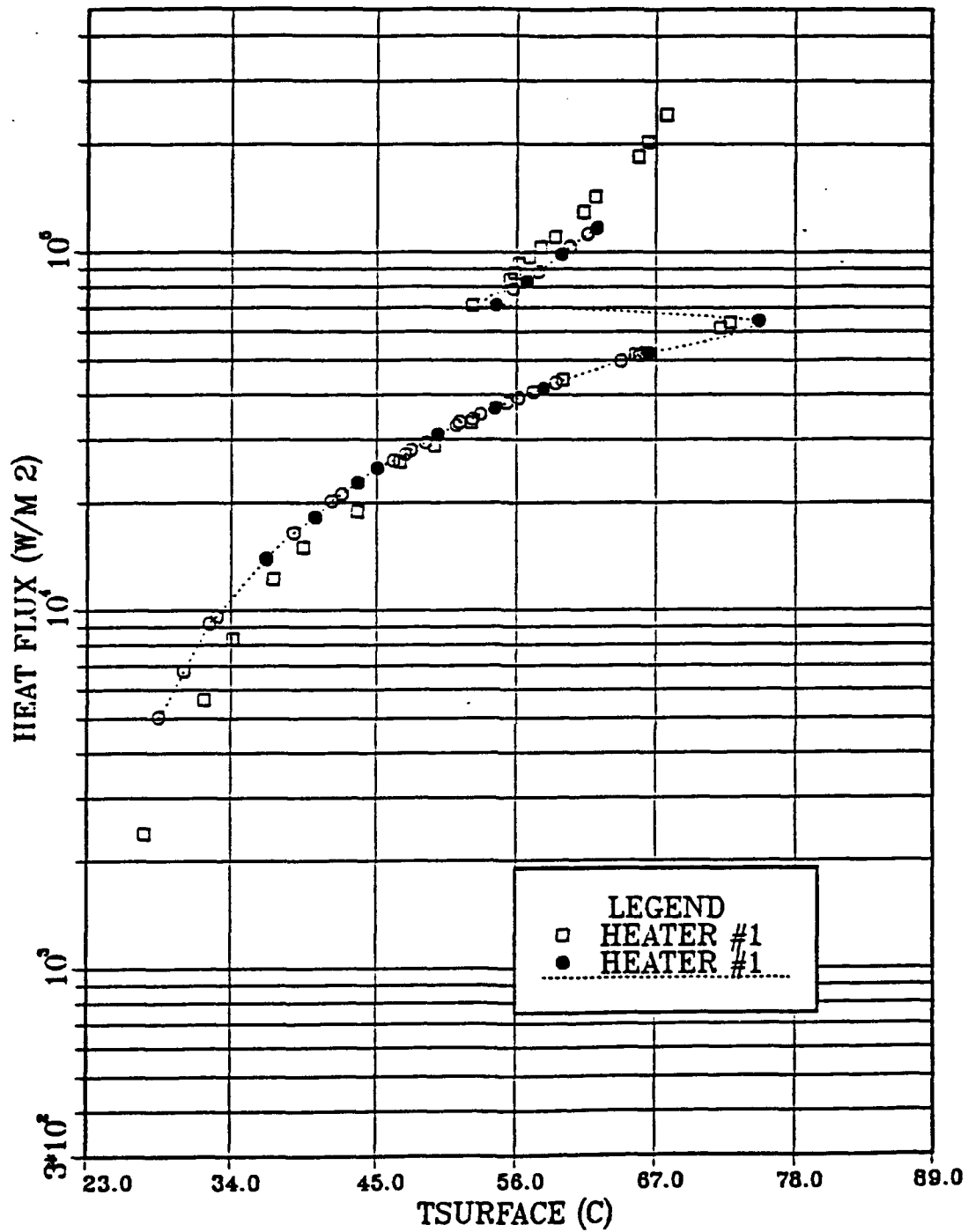
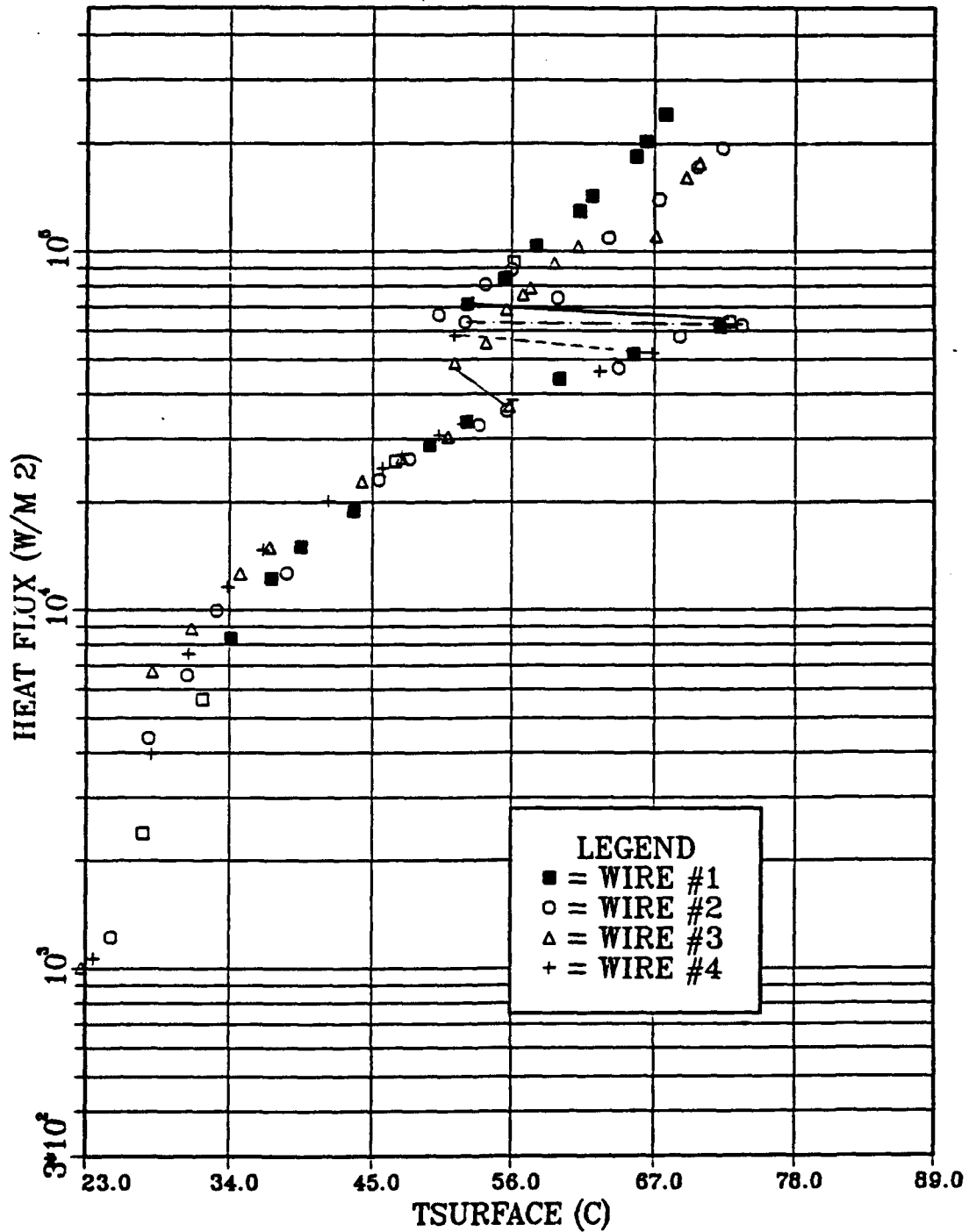


Figure 14. Number 1 at Different Times.

# INDIVIDUALLY POWERED



TBULK=23.5 C TSAT=56 C

Figure 15. All Wires Individually Powered.

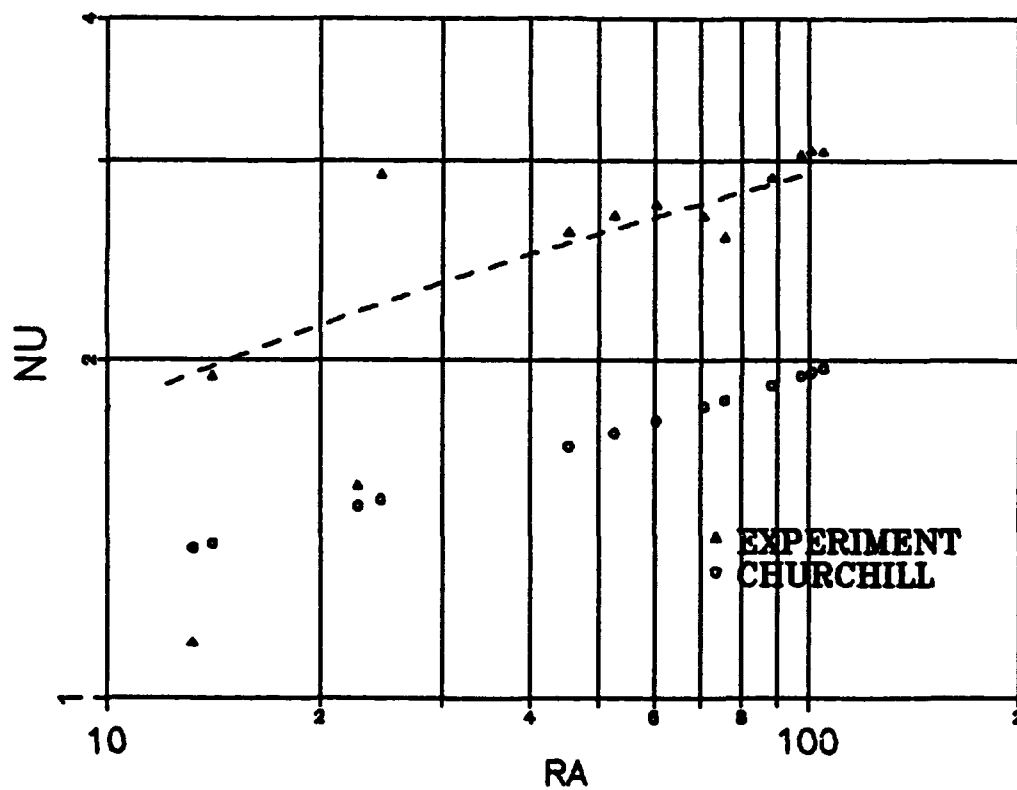


**Figure 16. Best Fit Experimental Data Compared with Churchill (1975) Correlation.**

# SUBCOOLING

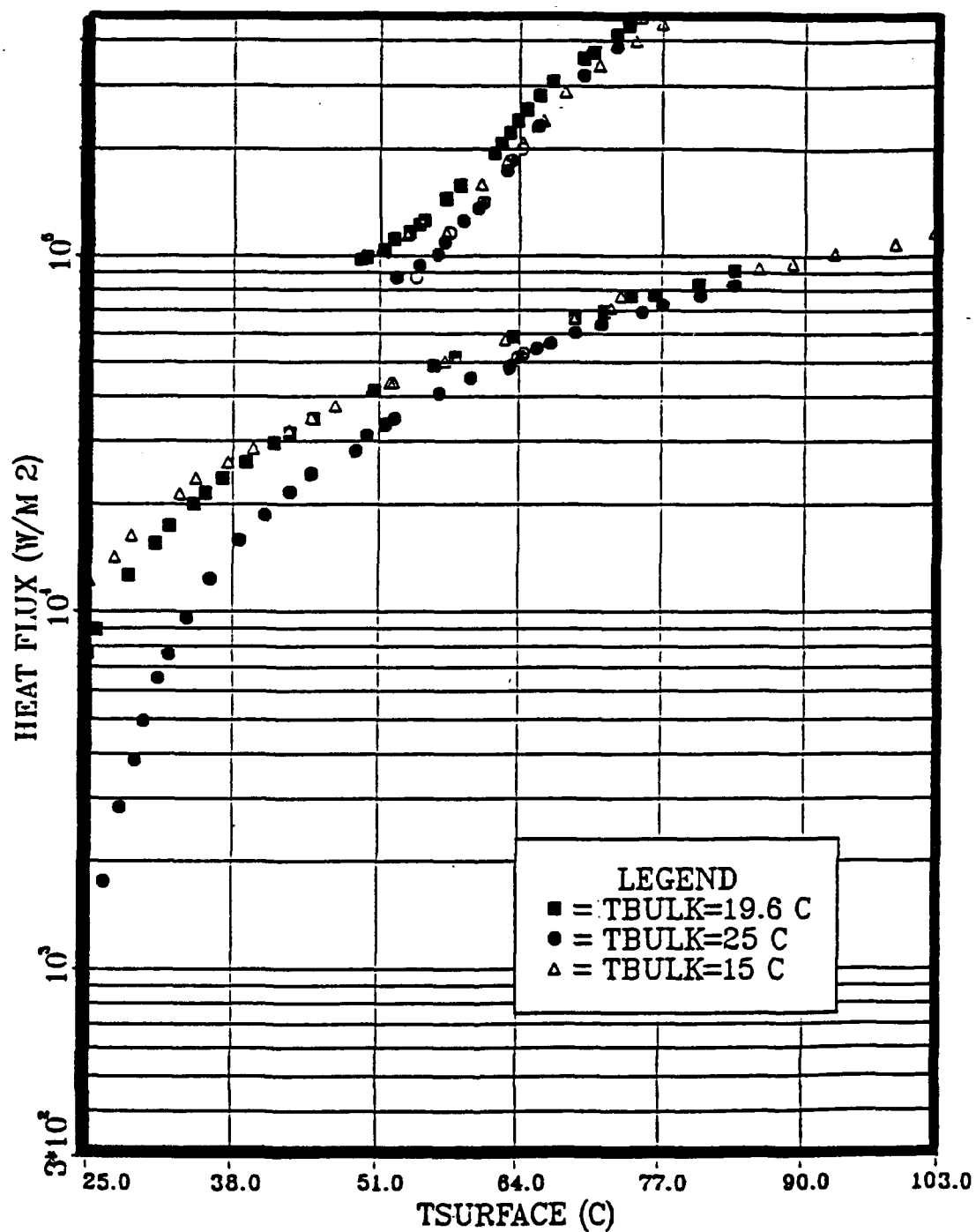


Figure 17. Subcooling.

# WIRE #4 AT CONS.HEAT FLUX

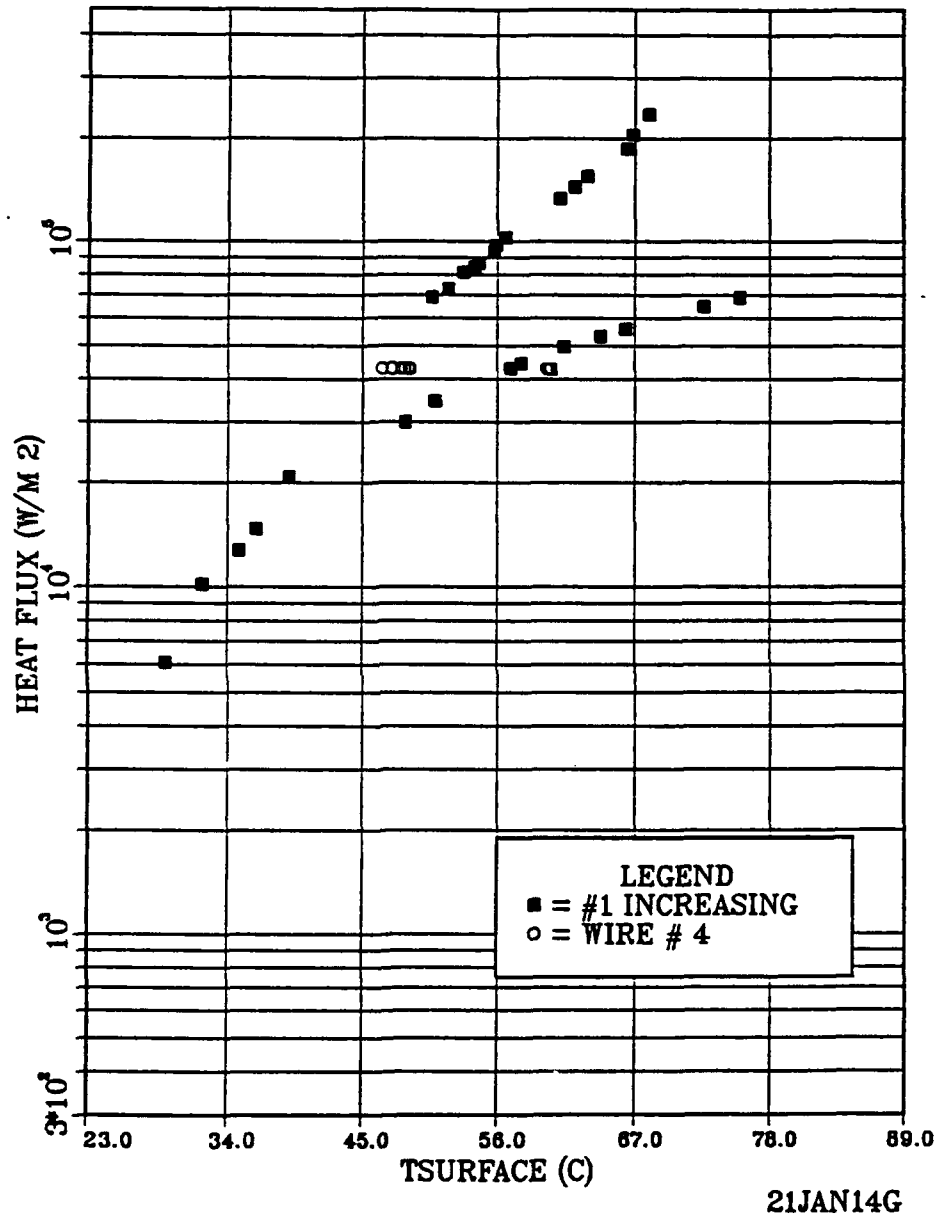


Figure 18. Pumping Effect with Wire Number 4 at 42,800 W/m<sup>2</sup>.



# WIRE 1 & 4(FIXED)

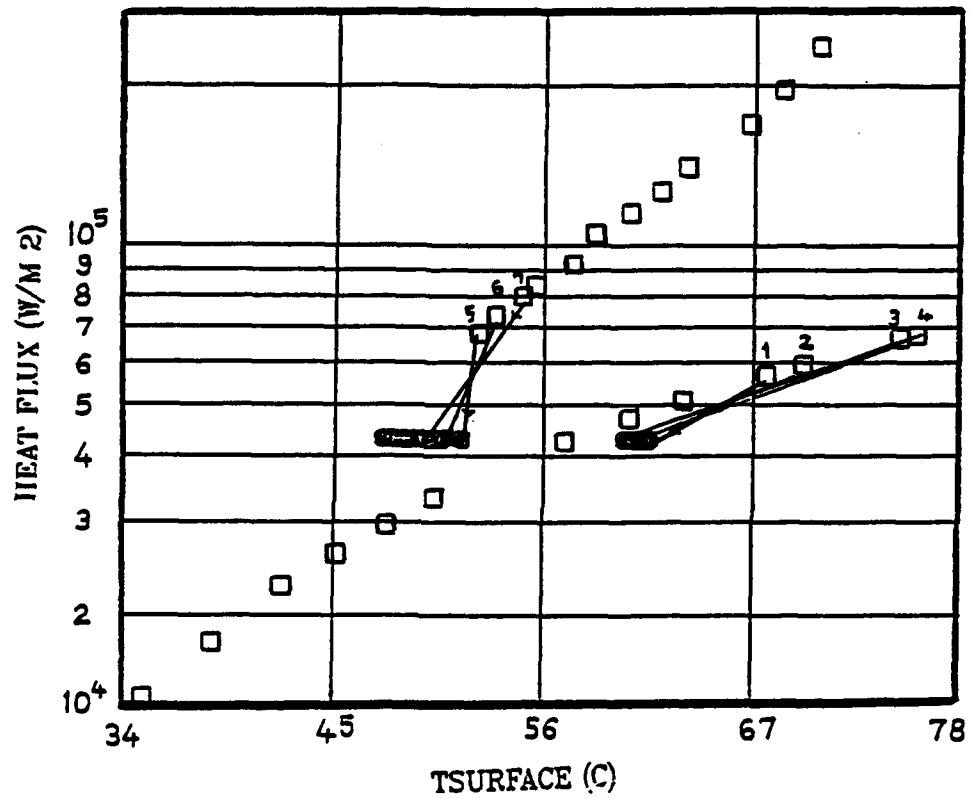


Figure 19. Pumping Effect with Wire Number 4  
(Detailed Figure).

# WIRE #4 AT CONST. HEAT FLUX

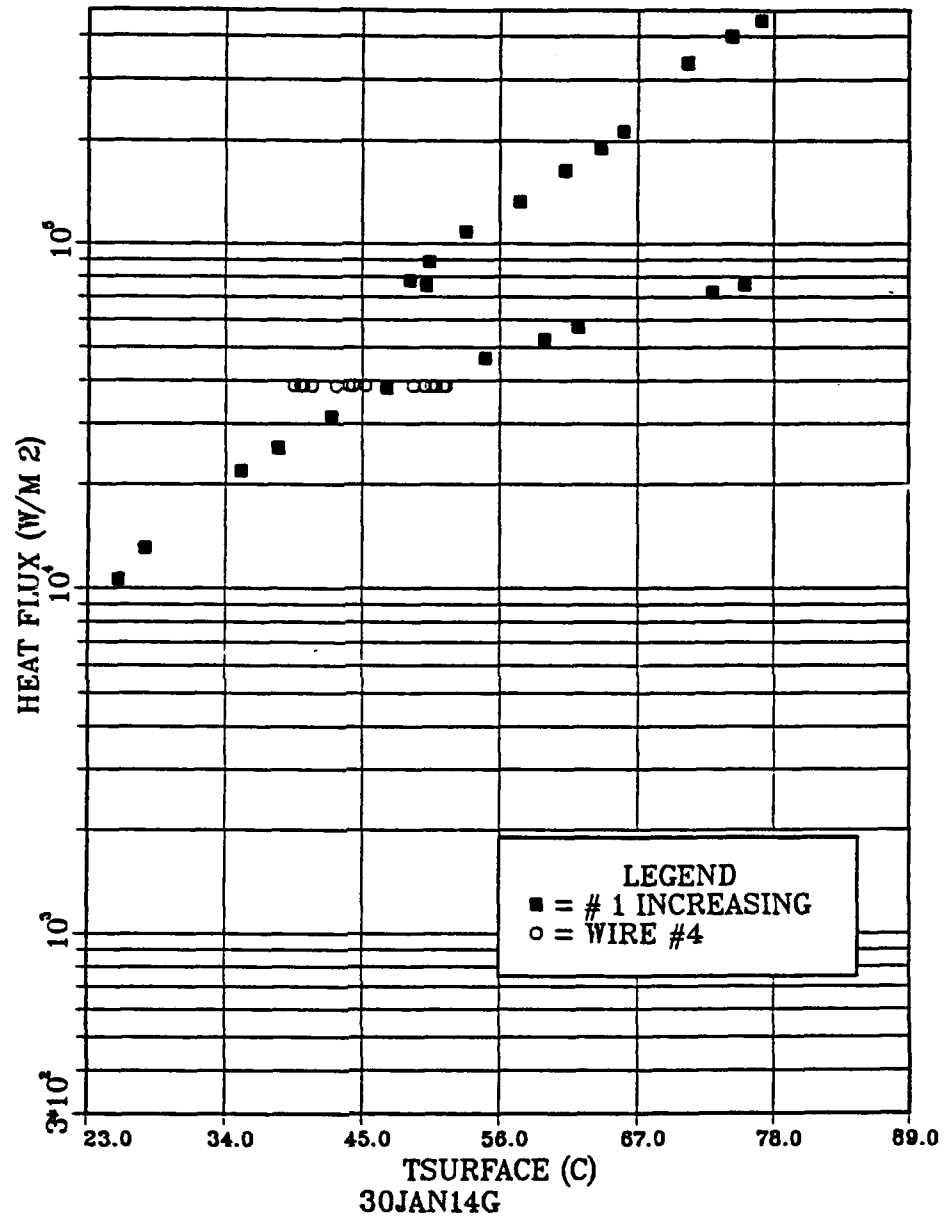


Figure 20. Wire Number 4 at Constant Heat Flux (38,600 W/m<sup>2</sup>) .

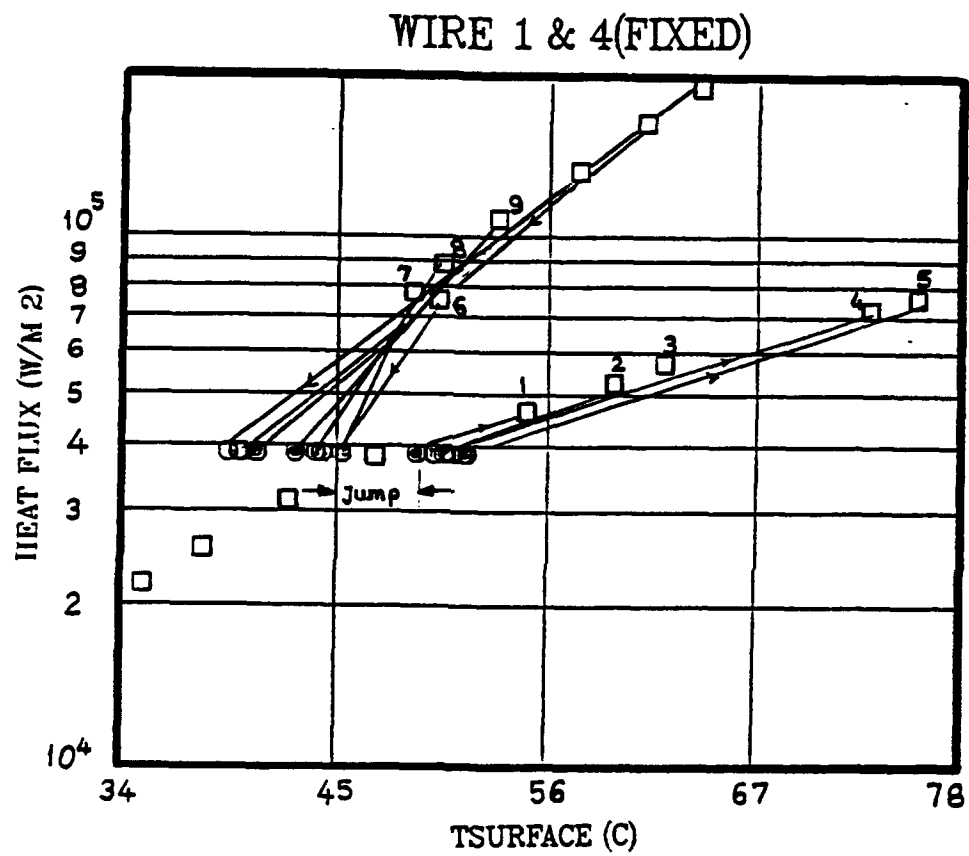


Figure 21. Detail of Figure 20.

# WIRE 1 & 3 (FIXED)

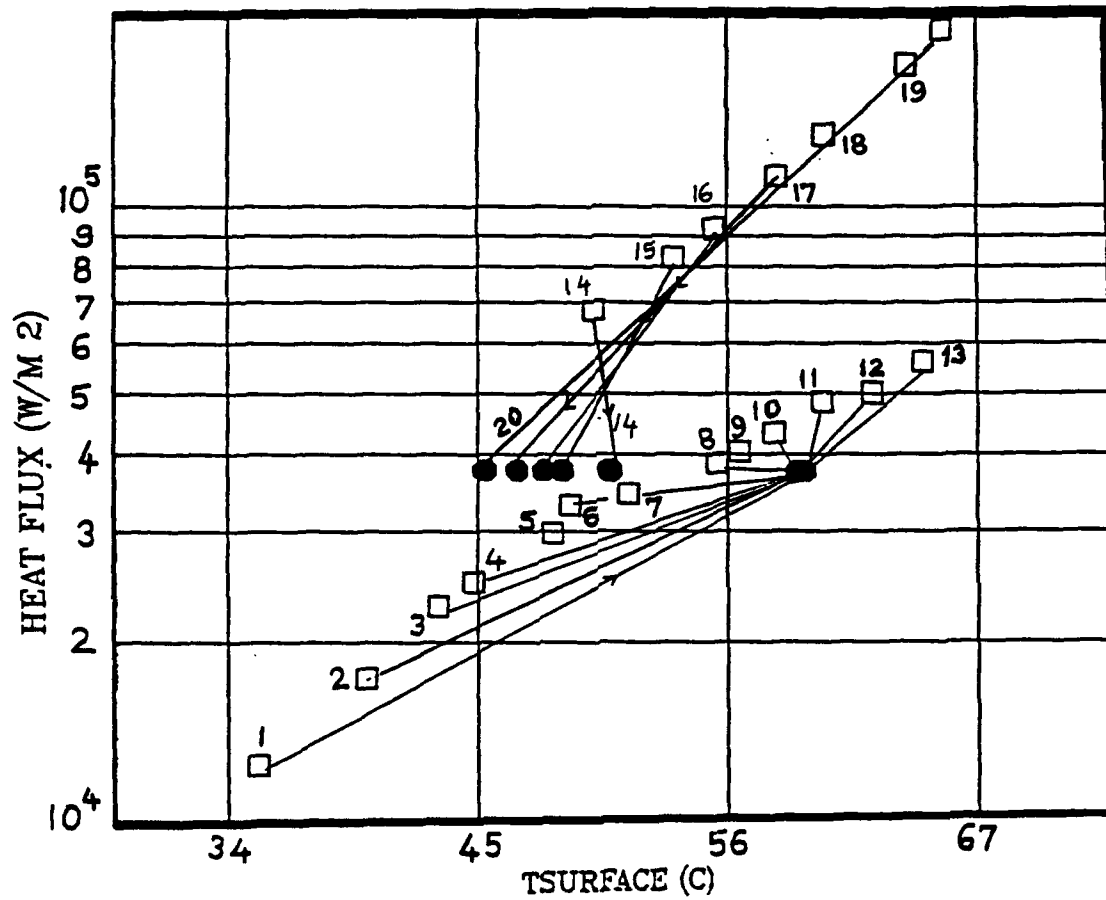


Figure 22. Wire Number 3 at Constant Heat Flux Value of 37,490 W/m².

# WIRE #3 AT CONS. HEAT FLUX

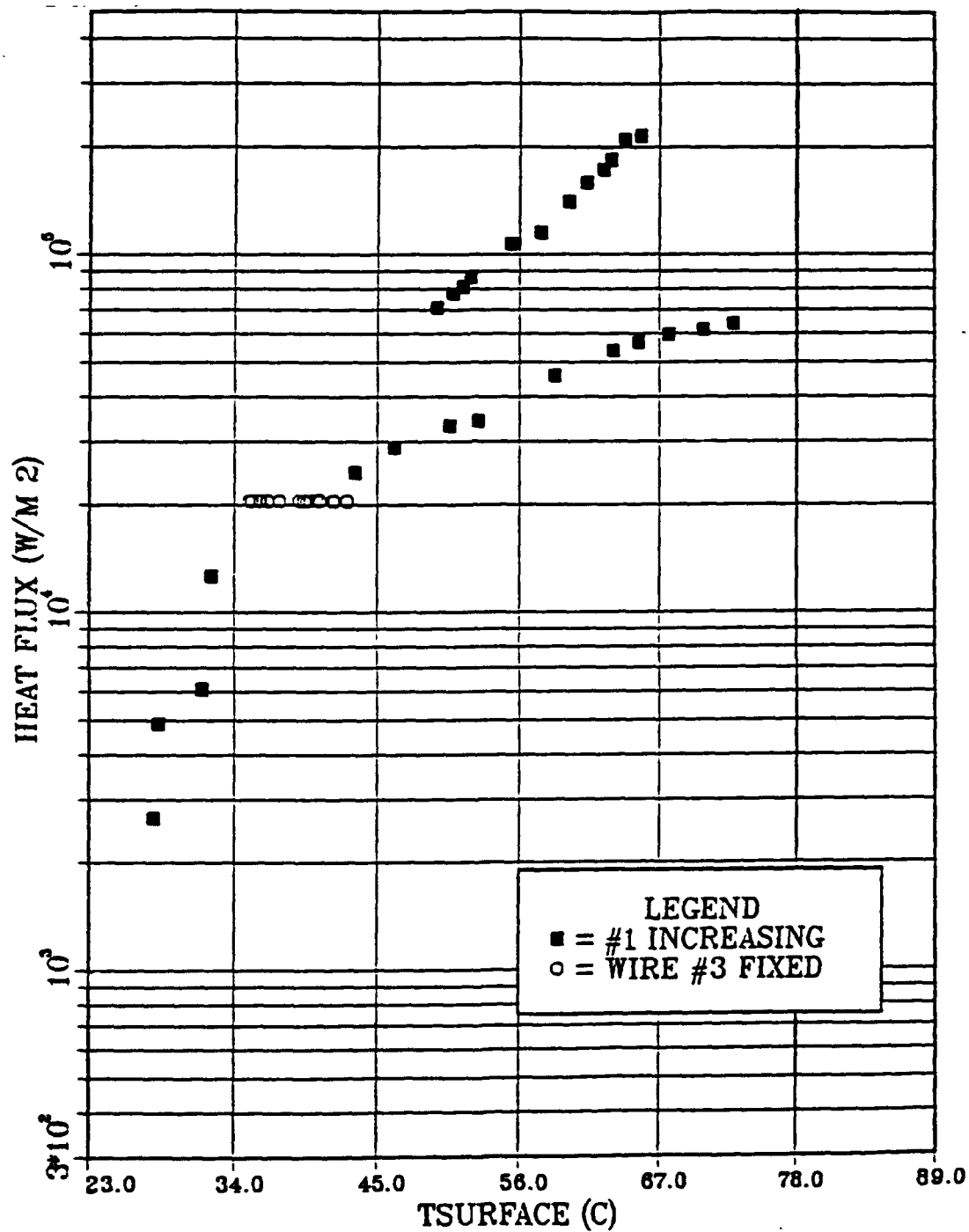


Figure 23. Wire Number 3 at 20,430 W/m².

# WIRE #2 AT CONS. HEAT FLUX

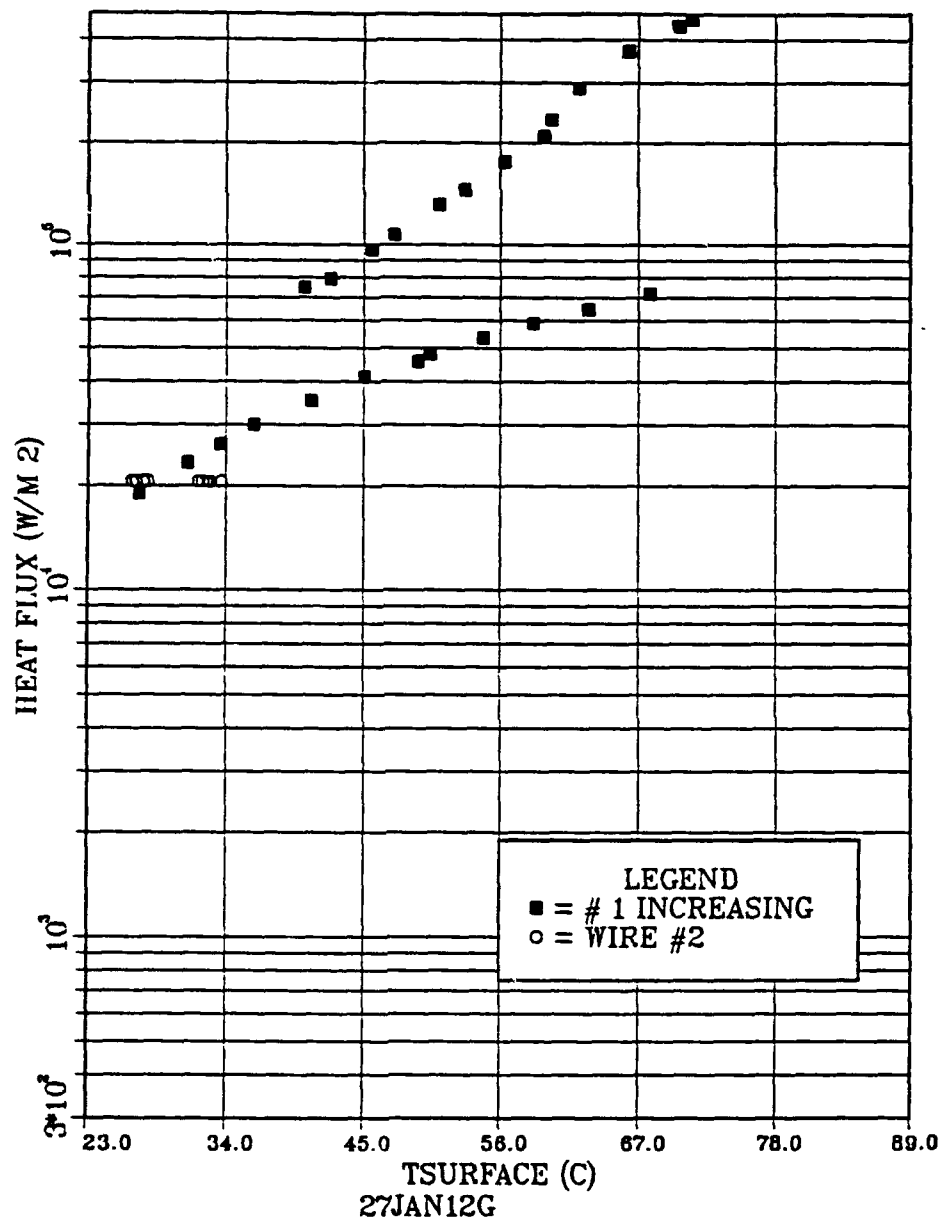


Figure 24a. Wire Number 2 at 20,530 W/m<sup>2</sup>.

# WIRE #2 AT CONS. HEAT FLUX

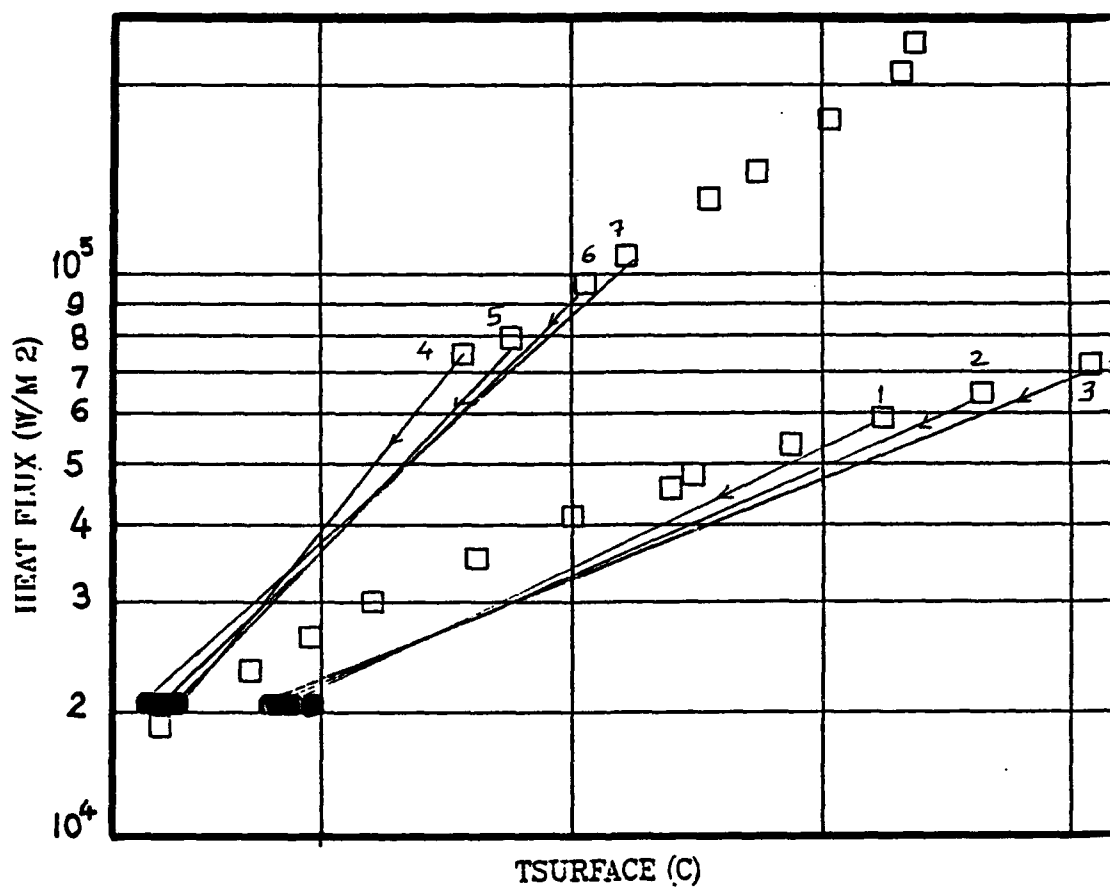


Figure 24b. Detail of Figure 24a.

# WIRE #2 AT CONS.HEAT FLUX

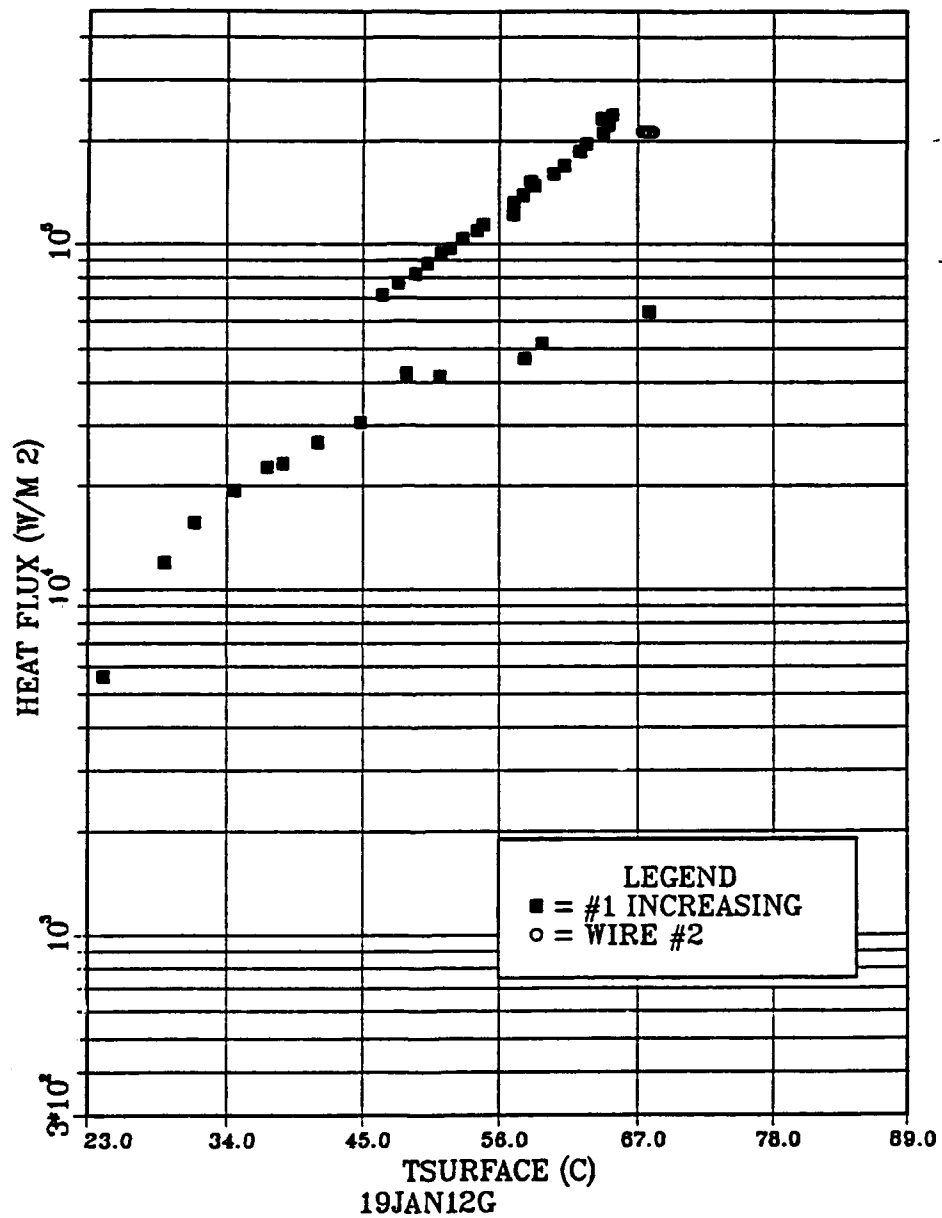


Figure 25a. Wire Number 2 Kept at 212,700 W/m<sup>2</sup>.



# WIRE #2 AT CONS.HEAT FLUX

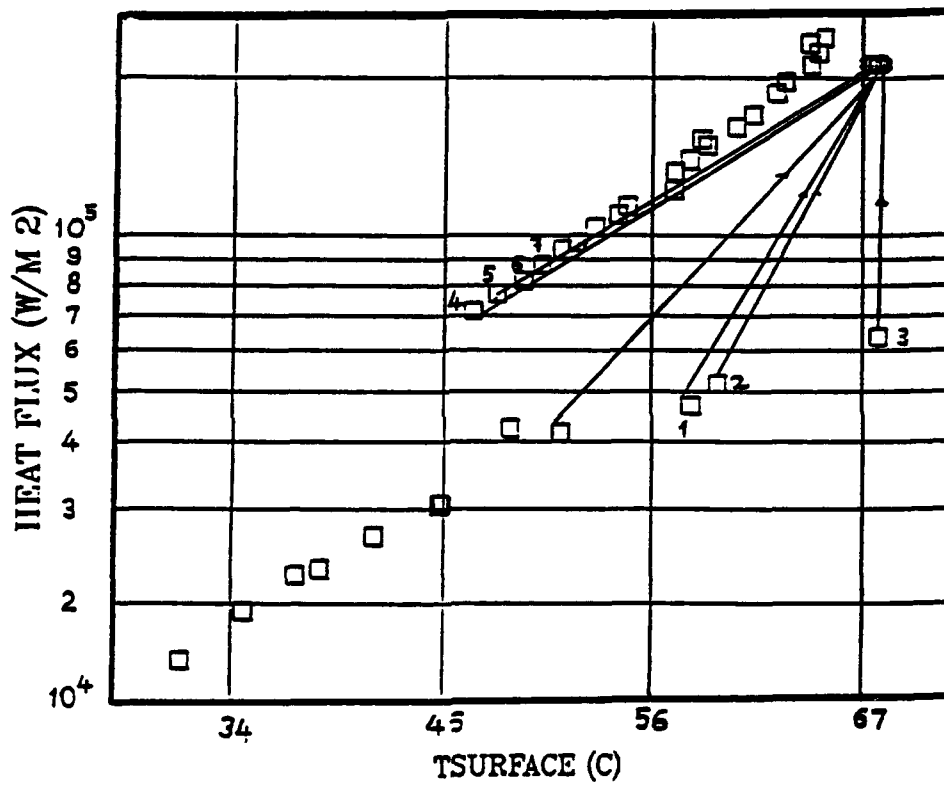


Figure 25b. Detail of Figure 25a.

# WIRE #3 AT CONS. HEAT FLUX

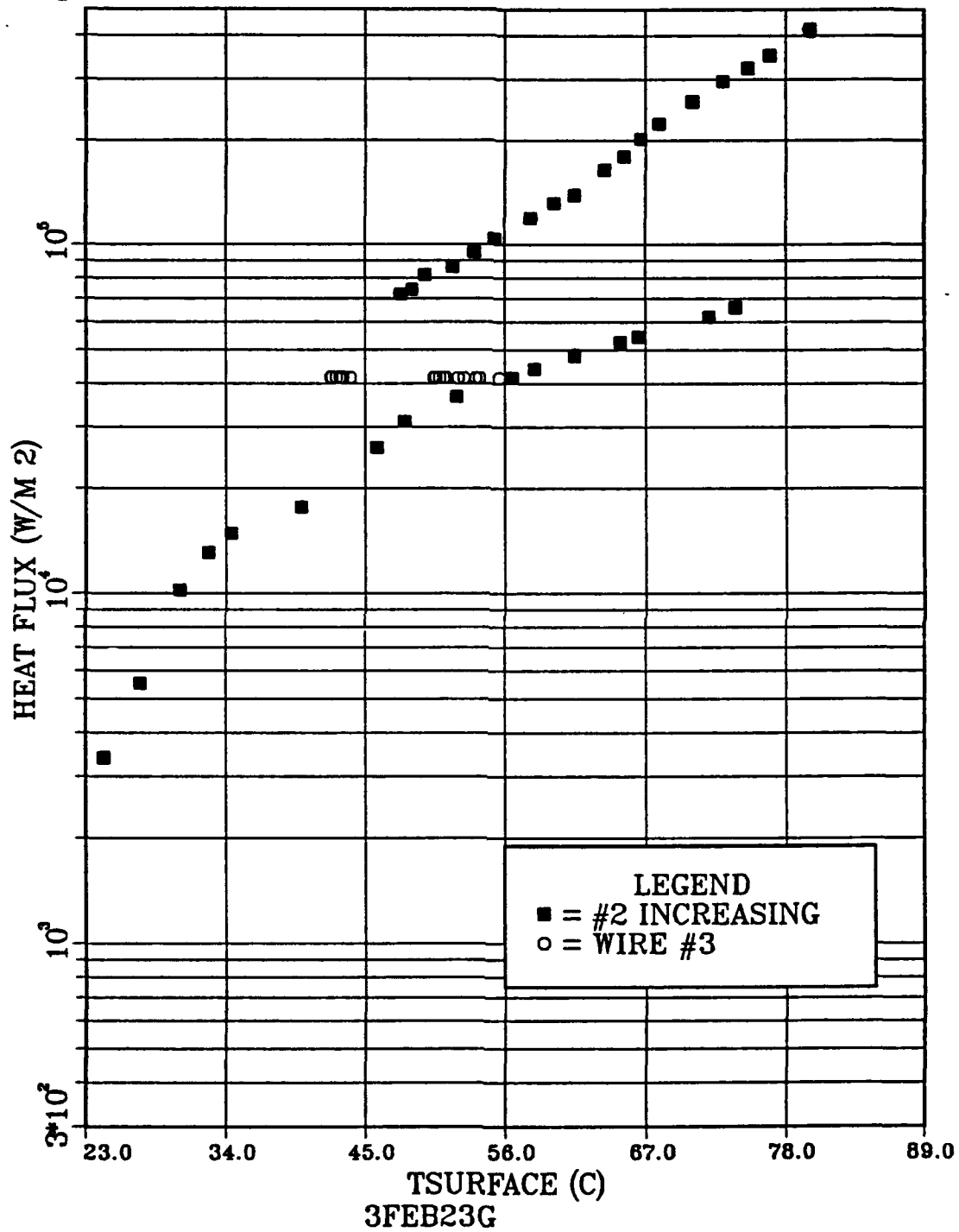


Figure 26. Wire Number 2 with Wire Number 3 at Constant Heat Flux.

## V. CONCLUSIONS

The figures give the idea of the pumping effects. When the pumping heater is powered progressively, the upper heater will react as indicated in the following.

- If the upper wire is located close to the lower pumper, it will meet most of the bubbles. It will lose some heat depending on how close it is.

- The initial heat flux value of the upper heater is also important. The amount of temperature jump which simultaneously occurs when the pumper has overshoot depends on how warm the upper wire is.

- If the upper heater already has bubbles, this means it had incipience before, and the bubbles will not help it lose more energy.

## **VI. RECOMMENDATIONS**

1. Use platinum wires rather than chromel wires to get better temperature measurement.
2. Before the start of each run, boil the pool for a sufficient time to degas the liquid.
3. Modify the software for taking data by adding a WAIT command to obtain the time function.
4. An addition of a foil type heater placed horizontally at the bottom of the chamber may help create a uniform temperature throughout the bulk fluid.
5. An extension of tygon tubing of about one foot length would take care of overflow and hydrostatic head determined by the liquid level inside the filling tank.
6. The present study deals with only subcooling effects. Saturated pool boiling should also be studied. In order to have constant temperature in the bulk fluid, the thermoelectric condensers and the bulk heaters can be run simultaneously.

## APPENDIX A. SAMPLE CALCULATIONS

### A. DETERMINATION OF INPUT POWER

For the sample calculations, the output values of wire number 1 were used:

$$\text{Power}(1) = \frac{\text{volt}(12)}{0.1} \text{ volt}(11)$$

where volt (12) and volt (11) are the voltages across the precision resistor and wire respectively.

$$= \left( \frac{0.0048}{0.1} \right) (1.988) = 0.96 \text{ Watts}$$

### B. CONVERSION FROM VOLTAGES TO TEMPERATURES (°C) FOR THERMOCOUPLES

The HP 3852 A Data Acquisition System channels 1-9 record the voltage readings in millivolts. The following polynomial formula is for copper constantan thermocouples.

$$\begin{aligned} T(^{\circ}\text{C}) = & 0.10086091 + (25727.9 * \text{emf}) - (767343.5 * \text{emf}^2) \\ & + (7802.5596 * \text{emf}^3) - (9247486589.6 * \text{emf}^4) + \\ & (6.98\text{E}11 * \text{emf}^5) - (2.66\text{E}13 * \text{emf}^6) + (3.94\text{E}14 * \text{emf}^7) \end{aligned}$$

Using thermocouple 1

$$\text{emf} = 0.000779 \text{ volt} \quad T = 19.72^{\circ}\text{C}$$

### C. CALCULATION OF WIRE TEMPERATURE

The calibration curve for the chromel wire (Kaye, 1976) yields the slope  $\epsilon$  of  $4.10^{-4}$  ohm/°C.

$$R = R_o [ 1 + \epsilon T - T_o ]$$

Here  $R_o$  and  $R$  are the resistances of the wire at the reference point and at any point to be measured  $R_o$  and  $ohm(1)$  are the corresponding variables used in the software.

$$T_s(1) = ((ohm(1)/R_o) - 1) / Kaye + T_o$$

where,

$$\begin{aligned} T_s(1) &= \text{wire temperature} \\ Kaye &= 0.0004 \text{ ohm/}^\circ\text{C constant slope} \\ T_o &= \text{wire reference temperature (}^\circ\text{C)}. \end{aligned}$$

$$\begin{aligned} T_s(1) &= (((4.1009/4.075) - 1) / 4E-4) + 19.64 \\ &= 35.5^\circ\text{C} \end{aligned}$$

#### D. CALCULATION OF THE AVERAGE BULK TEMPERATURE

The average temperature of the liquid was simply the arithmetic average of the three thermocouple values immersed in the bulk fluid.

$$\begin{aligned} T_{bulk} &= (T(1) + T(2) + T(3)) / 3 \\ &= (19.9 + 19.54 + 19.6) / 3 = 19.68^\circ\text{C} \end{aligned}$$

#### E. DETERMINATION OF HEAT FLUX

$$HFLUX(1) = \frac{Power(1)}{AREA}$$

where,

$$\begin{aligned} AREA &= \pi * D * L = (3.1415926) D L \\ D, L &= \text{Diameter and length of the wire.} \\ AREA &= (3.1415926) (0.005) (0.0254^2) (3) = 3.04E-5 \text{ m}^2 \end{aligned}$$

$$HFLUX = \frac{2.355}{3.04E-5} = 77460 \text{ W / m}^2$$

## **F. FLUID PROPERTIES DETERMINATION**

### **1. Thermal Conductivity $k$ (W/m°C)**

From Figure 5 of the 3M Corporation Flourinert Product Manual, the thermal conductivity coefficient curves have been determined to be

$$K = (0.6033 - 0.00115 * T_b) / 10 \quad \frac{1 \text{ mW}}{\text{Cm}^\circ\text{C}} = 0.1 \frac{\text{W}}{\text{mK}}$$

at  $T_b = 50^\circ\text{C}$  it yields 0.0545 W/m.

### **2. Liquid Density $\rho$ (kg/m³)**

Using the expression in Table 4B and constants presented in Table 4C of the Product Manual yields

$$\rho = (1.740 - 0.00261 T_b) * 1000$$

$T_b$  film temperature must be in units of  $^\circ\text{C}$ . At  $T_b = 50^\circ\text{C}$  this yields  $\rho = 1609.5 \text{ kg/m}^3$ .

### **3. Kinematic Viscosity $\nu$ (m²/s)**

From Figure (3) and determining a 4th order curve fit yields

$$\nu = (0.54 - 0.0116 * T_b + 0.0002085 * T_b^2) * 1\text{E-}6$$

at  $T_b = 50^\circ\text{C}$  this yields  $\nu = 4.8\text{E-}7 \text{ m}^2/\text{s}$ .

### **4. Density of Vapor $\rho_v$ (kg/m³)**

From Table 13A of the Product Manual, values for vapor density can be taken.

For the range of 20-80°C the data can be approximated as a fourth order polynomial.

$$V_v = (246 - 10.93 * T_b + 0.213 * T_b^2 - 0.00193 * T_b^3 + 6.55\text{E-}6 * T_b^4) / 338$$

$T_b = 50^{\circ}\text{C}$  it yields

$\rho_v = 10.67 \text{ (kg/m}^3\text{)}$

where  $V_v = \frac{1}{\rho_v}$ .

#### **5. Specific Heat $C_p$ (J/kg $^{\circ}\text{C}$ )**

For all Flourinert Electrochemicals (Figure 4)

$$C_p = (0.241111 + 3.70374\text{E-}4 * T_b) * 4186$$

at  $T = 50^{\circ}\text{C}$ . Calculation yields 1086.7 J/kg $^{\circ}\text{C}$ .

#### **6. Thermal Diffusivity $\alpha$ (m $^2$ /s)**

$$\alpha = k/\rho C_p$$

at  $T = 50^{\circ}\text{C}$ , calculation yields 3.115E-8 m $^2$ /s.

#### **7. Thermal Expansion Coefficient $\beta$ (1/ $^{\circ}\text{C}$ )**

Table 4B in the Product Manual shows

$$\beta = 0.00261 / (1.740 - 0.00261) * T_b)$$

at  $T = 50^{\circ}\text{C}$ . Calculation results in 0.00162 (1/ $^{\circ}\text{C}$ ).

#### **8. Prandtl Number (Pr)**

$$Pr = \nu/\alpha$$

at  $T=50^{\circ}\text{C}$ . This yields  $Pr = 15.4$

#### **9. Calculation of Latent Heat $hfg$ (J/kg)**

Table 13A of the Product Manual shows the values can be approximated by a linear equation.

$$hfg = (8057 - 22.73 * T_b) * 10.79$$

where 10.79 is the conversion factor from Cal/Mole to (J/kg).

At  $T = 50^{\circ}\text{C}$  calculation yields 74672 (J/kg).



## APPENDIX B. UNCERTAINTY ANALYSIS

### A. UNCERTAINTY IN AREA

$$\omega_D = .0001 \text{ inches}$$

$$\omega_L = \pm 0.010 \text{ inches}$$

$$A = \pi D L$$

where:

$$D = \text{Wire diameter}$$

$$L = \text{Length of heater wire}$$

$$A = (3.141593 * 0.005 * 3)$$

$$= 0.0471 \text{ in}^2$$

$$= 3.04 * 10^{-5} \text{ m}^2$$

$$\frac{\partial A}{\partial D} = (\pi L)$$

$$\frac{\partial A}{\partial L} = (\pi D)$$

Therefore,

$$\omega_A = \left[ (\pi L \omega_D)^2 + (\pi D \omega_L)^2 \right]^{1/2}$$

$$\frac{\omega_A}{A} = \left[ \left( \frac{\omega_D}{D} \right)^2 + \left( \frac{\omega_L}{L} \right)^2 \right]^{1/2}$$

$$= \left[ \left( \frac{0.0001}{0.005} \right)^2 + \left( \frac{0.020}{3} \right)^2 \right]^{1/2}$$

$$\frac{\omega_A}{A} = 0.021 \text{ or } 2.1\%$$

$$\omega = 6.38 \times 10^{-9} \text{ in}^2 = 9.89 \times 10^{-4} \text{ m}^2$$

#### B. UNCERTAINTY IN POWER

$$\omega_I = \pm 0.05 \text{ Ampere} \quad \begin{array}{l} \text{Taken from (Hazard, 1986)} \\ \text{calculation)} \end{array}$$

$$\omega_V = \pm 0.5 \text{ volt}$$

$$Q = V I$$

$$\frac{\partial Q}{\partial V} = I$$

$$\frac{\partial Q}{\partial I} = V$$

$$\omega_Q = [ (I \omega_V)^2 + (V \omega_I)^2 ]^{1/2}$$

$$\frac{\omega_Q}{Q} = \left[ \left( \frac{0.05}{7.46} \right)^2 + \left( \frac{0.001}{0.018} \right)^2 \right]^{1/2}$$

$$= 0.059 \text{ or } 5.9\%$$

### C. UNCERTAINTY IN HEAT FLUX

$$q = \frac{Q}{A}$$

$$\frac{\partial q}{\partial Q} = \frac{1}{A}$$

$$\frac{\partial q}{\partial A} = -\frac{Q}{A^2}$$

$$\omega_q = \left[ \left( -\frac{Q}{A^2} \omega_A \right)^2 + \left( \frac{1}{A} \omega_Q \right)^2 \right]^{1/2}$$

$$\frac{\omega_q}{q} = \left[ \left( \frac{\omega_A}{A} \right)^2 + \left( \frac{\omega_Q}{Q} \right)^2 \right]^{1/2}$$

$$= [ 0.021^2 + 0.059^2 ]^{1/2}$$

$$= 0.062 \text{ or } 6.2\%$$

#### D. UNCERTAINTY IN TEMPERATURE

Using thermocouples:

<u>Variable</u>	<u>Uncertainty</u>
Voltmeter resolution	0.026°C
	1.0 mv resolution
Ice reference bath	0.05°C
Temperature	
Polynomial Temperature	0.00663°C RMS
Conversion	
R	1.0%

$$\begin{aligned}\omega T_b &= [ (\omega_{VR})^2 + (\omega_{IB})^2 ]^{1/2} + \omega_{curve} \\ &= [ (0.0025)^2 + (0.05)^2 ]^{1/2} + 0.00663 \\ \omega T_b &= 0.063 \text{ or } 6.3\%\end{aligned}$$

#### E. UNCERTAINTY OF WIRE SURFACE TEMPERATURE

From the calibration formula

$$R = R_o [ 1 + \epsilon \Delta T ] \quad (1)$$

where,

$$\begin{aligned}\Delta T &= T_s - T_b \\ \epsilon &= \text{Slope of the calibration curve} \\ T_b &= \text{Bulk fluid temperature.}\end{aligned}$$

From (1)

$$T_s = \left( \frac{R}{R_o} - 1 \right) / \epsilon + T_b \quad \text{For: } T_s = 44.14^\circ\text{C}$$

$$\frac{\partial T_s}{\partial T_b} = 1$$

$$T_b = 23.9^\circ\text{C}$$

$$\frac{\partial T_s}{\partial R} = \frac{1}{R_o \epsilon}$$

$$\epsilon = 0.0004 \pm 12\%$$

$$\frac{\partial T_s}{\partial R_o} = \frac{-R}{R_o^2 \epsilon}$$

$$R_o = 3.88 \Omega$$

$$\frac{\partial T_s}{\partial \alpha} = \frac{1}{\epsilon^2} \left( 1 - \frac{R}{R_o} \right)$$

$$R = 3.91 \Omega$$

$$\omega_R = \omega_{R_o} = 0.01$$

$$\omega T_s =$$

$$\left\{ \left( \frac{\partial T_s}{\partial T_b} \right)^2 (\omega T_b)^2 + \left( \frac{\partial T_s}{\partial R_o} \right)^2 (\omega R_o)^2 + \left( \frac{\partial T_s}{\partial R} \right)^2 (\omega_R)^2 + \left( \frac{\partial T_s}{\partial \epsilon} \right)^2 (\omega_\epsilon^2)^2 \right\}^{1/2}$$

$$\begin{aligned} \omega T_s &= \{ 1 (0.063)^2 + (6.49)^2 + 6.44^2 + 2.31 \}^{1/2} \\ &= 9.43^\circ\text{C} \end{aligned}$$

#### F. UNCERTAINTY IN $\Delta T$

Where  $\Delta T = T_s - T_b$

$$\frac{\partial \Delta T}{\partial T_s} = 1$$

$$\frac{\partial \Delta T}{\partial T_b} = -1$$

$$\omega_{\Delta T} = \left[ \left( \frac{\partial \Delta T}{\partial T_s} \omega_{T_s} \right)^2 + \left( \frac{\partial \Delta T}{\partial T_b} \omega_{T_b} \right)^2 \right]^{1/2}$$

$$\frac{\omega_{\Delta T}}{\Delta T} = \left[ \left( \frac{W_{T_s}}{T_s} \right)^2 + \left( \frac{W_{T_b}}{T_b} \right)^2 \right]^{1/2}$$

$$\frac{\omega_{\Delta T}}{\Delta T} = \left[ \left( \frac{9.43}{44.14} \right)^2 + \left( \frac{0.063}{23.99} \right)^2 \right]^{1/2}$$

$$= 0.21 \text{ or } 21\%$$

$$\omega_{\Delta T} = 0.21 (44.14 - 23.99)$$

$$= 4.3^\circ\text{C}$$

#### G. UNCERTAINTY IN HEAT TRANSFER COEFFICIENT

$$h = \frac{q}{\Delta T} \quad \text{q is the heat flux}$$

$$\frac{\partial h}{\partial q} = \frac{1}{\Delta T} \quad q = 20190 \text{ W/m}^2$$

$$\frac{\partial h}{\partial \Delta T} = \frac{-q}{\Delta T^2}$$

$$\Delta T = 44.14 - 23.99$$

$$\omega_h = \left[ \left( \frac{1}{\Delta T} \omega_q \right)^2 + \left( -\frac{q}{\Delta T^2} \omega_{\Delta T} \right)^2 \right]^{1/2} = 20.15^\circ\text{C}$$

$$\frac{\omega_h}{h} = \left[ \left( \frac{\omega_q}{q} \right)^2 + \left( \frac{\omega_{\Delta T}}{\Delta T} \right)^2 \right]^{1/2}$$

$$= \left[ (0.062)^2 + \left( \frac{4.3}{20.15} \right)^2 \right]^{1/2}$$

$$= 0.222 \text{ or } 22\%$$

### APPENDIX C. CALIBRATION OF CHROMEL WIRES

The chromel wires of about 3 inch length were immersed in a Rosemount constant temperature distilled water bath, and were compared with a platinum resistance thermometer as a standard. The temperature was raised from 30°C to 90°C in increments of about five degrees. At each increment, the temperature was allowed to stabilize for five minutes, then measured using a Newport digital thermistor device for the 0.005 inch diameter chromel wire. All recorded data are presented in the following table. The corresponding best fit line is also presented on the graph. Two sets of data were taken at different times.

Thermistor (C)	T/C	Resistance (Ohm)
29	30.2	4.74
38.3	39.7	4.76
49.5	51	4.78
61.9	63.4	4.8
76.2	77.2	4.83
87.7	88.4	4.85
52.3	53.8	4.79
57.5	59.1	4.8
60.5	62	4.8
68.3	69.6	4.81
70.7	72	4.82
71.3	72.4	4.82
86.2	86.9	4.84



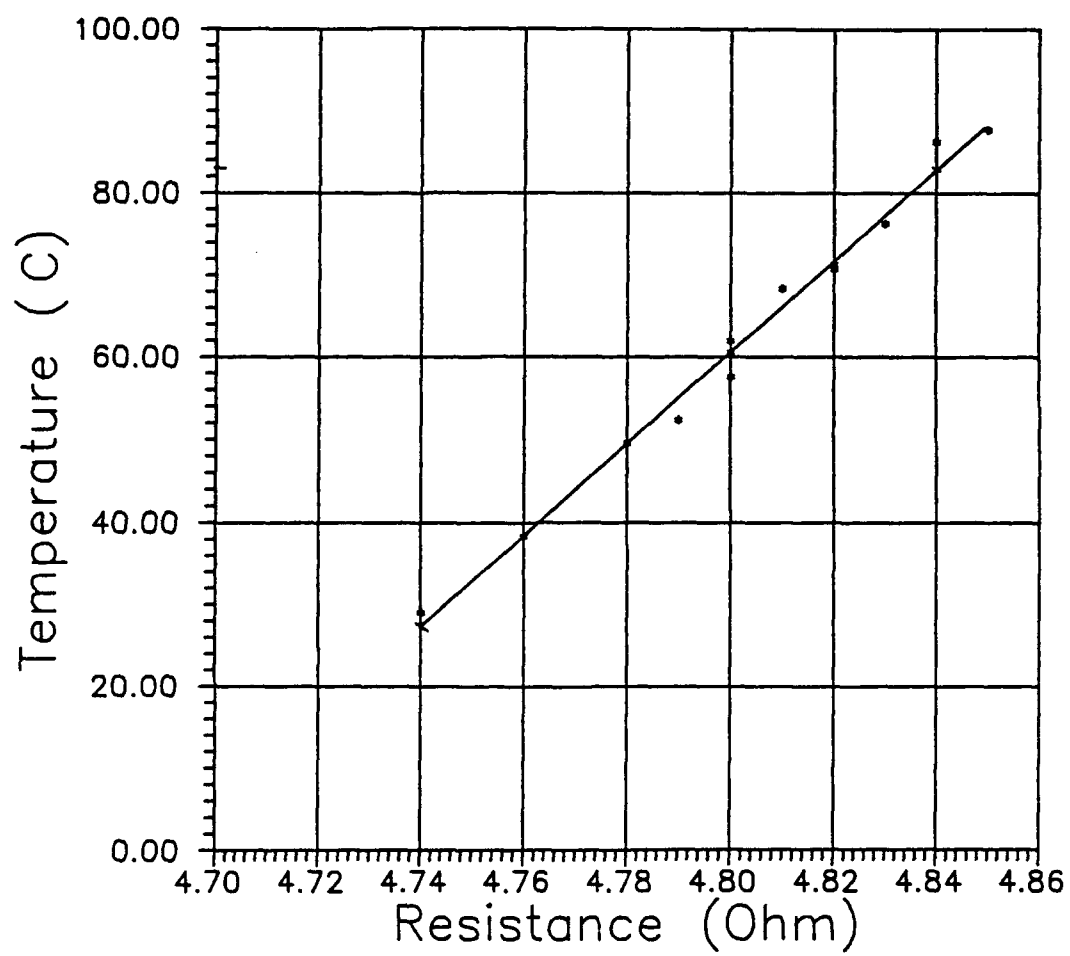


**Figure C1. Chromel Wire Calibration.**

#### APPENDIX D. SOFTWARE

Software written in the BASIC language converts voltage measurements into temperature values for the bulk fluid, ice reference, and coolers inside the thermocouples. It uses the  $\alpha$  value of 0.0004 Ohm/°C to calculate the surface temperature offered by Kaye (1976). The printed output covers bulk fluid, wire surface temperatures and heat flux.

A FORTRAN program reads the output values created by the previous program and calculates liquid properties  $R_a$ ,  $Nu$ , and  $C_{sf}$ .

The GRAPHER program graphs the data and prints it using a HP-7440A Plotter.

Initial experiment data was fed into EASYPLOT software on the Naval Postgraduate School's main frame computer via floppy diskettes.

```

11  OPTION BASE 1
12  BEEP
13  PRINT "INPUT DATE"
14  INPUT Tarihs
15  PRINT " INPUT TIME "
16  INPUT Zam
18  IPRINT "SCANNING MEAS"
19  REAL Emf(7),T(7),D(8),Volt(11:19),Power(4),Hflux(4),Ts(4),Ohm(4)
20  REAL Sumo
25  OUTPUT 709;"CONFMEAS DCV,101-107,USE 0"
26  FOR I=1 TO 7
27  ENTER 709;Emf(I)
29  IPRINT I;Emf(I)
30  NEXT I
31  OUTPUT 709;"CONFMEAS DCV,111-119,USE 0"
32  FOR I=11 TO 19
33  ENTER 709;Volt(I)
35  IPRINT I;Volt(I)
36  NEXT I
37  D(1)=-.10086091
38  D(2)=-25727.9
39  D(3)=-767345.8
40  D(4)=-78025596
41  D(5)=-9247486589
42  D(6)=-6.98E+11
43  D(7)=-2.66E+13
44  D(8)=-3.94E+14
45  FOR I=1 TO 7
46  Sumo=0.
47  FOR J=1 TO 8
48  Sumo=Sumo+D(J)*Emf(I)^(J-1)
49  NEXT J
50  T(I)=Sumo
51  Tb=(T(2)+T(3)+T(1))/3
52  NEXT I
53  PRINT "DATE :";Tarihs
54  PRINT "TIME : ";Zam
55  PRINT "T";1,T(1);" C  UPPER PORTION OF THE FLUID"
56  IPRINT USING "T";1,DD.D;T(1);" C  UPPER PORTION OF THE FLUID"
57  PRINT "T";2,T(2);" C  LOWER PORTION OF THE FLUID"
58  PRINT "T";3,T(3);" C  LOWER PORTION OF THE FLUID"
59  PRINT "T";4,T(4);" C  TE COOLER INSIDE AL. PLATE"
60  PRINT "T";5,T(5);" C  TE COOLER INSIDE AL. PLATE"
61  PRINT "T";6,T(6);" C  AMBIENT (ROOM TEMPERATURE)"
    TEMPERATURE"

```

```

62 PRINT "T";7,T(7);"C  ICE (REFERENCE TEMPERATURE)"
63 INEXT I
64 PRINT "TBULK=";Tb
65 !power calculations*****
66 Power(1)=(Volt(12)/.1)*Volt(TF)
67 Power(2)=(Volt(17)/.1)*Volt(16)
68 Power(3)=(Volt(17)/.1)*Volt(16)
69 !heater surface area calculations
70 !*****
71 Dia=.005*.0254
72 Al=3*.0254
73 Alan=(3.1415926)*Dia*Al
74 !heat flux calc.
75 !*****
76 Hflux(1)=Power(1)/Alan
77 Hflux(2)=Power(2)/Alan
78 Hflux(3)=Power(3)/Alan
79 PRINT "power1=";Power(1)
80 PRINT "power2=";Power(2)
81 PRINT "power3=";Power(3)
82 !*****
83 Ohm(1)=Volt(11)/(Volt(12)/.1)
84 Ohm(2)=Volt(14)/(Volt(16)/.1)
85 Ohm(3)=Volt(16)/(Volt(17)/.1)
86 PRINT "OHM2=";Ohm(2)
87 PRINT "OHM1=";Ohm(1)
88 PRINT "OHM3=";Ohm(3)
89 Dt=Tb-Ta
90 ! Ta IS THE TEMP OF BULK FLUID Tb WHEN POWER OFF
91 ! Ro IS THE RESIS. OF CHROMEL WIRE ACTUALLY IT IS
92 ! THE OHM(1) VALUE WHEN THE BULK FLUID TEMP (Tb=Tamb) AND POWER OFF
93 ! ( POWER OFF MEANS Power(1)*0.0084 and it is obtained by setting )
94 ! POWER(4)*0.0088
95 ! R01=4.069 R04=3.7981
96 ! (VIZ 40 V Supplyist to 00.1 0.10 position WHEN 1&4 INSERTED
97 ! Kye is the value of the calibration slope Ref[S.M YOU et al]
98 ! *****
99 Ta=Tb
100 Ro1=4.069
101 Ro3=3.7981
102 Kye=.0004
103 R=4.069*(1+.0004*Dt)
104 Ts(1)=(((Ohm(1)/Ro1)-1)/Kye)+Ta
105 Ts(3)=(((Ohm(3)/Ro3)-1)/Kye)+Ta
106 Tfilm=(Tb+Ts(4))/2
107 PRINT "TS1=";Ts(1), " HFLUX ";Hflux(1)
108 PRINT "TS3=";Ts(3), " HFLUX3 ";Hflux(3)
109 PRINT "T film ";Tfilm
110 END

```

```

* *****
* PARAMETER ( N=28 )
* INTEGER I
* REAL TS(N), TB(N), HF(N), NU(N), RA(N), NUC(N), TF(N), TF1(N), BETA(N)
+ , DENF(N), DENV(N), KINV(N), CP(N), K(N), HFG(N), ALF(N), PR(N)
+ , SURT(N), RAYD(N), RAYFB(N), NUSEX(N), NUSC(N), DIA, G, V(N)
+ , MU(N), Y(N), X(N), WS(N), TSAT, CSF(N)
* *****
* READ Tsurface, Heat Flux, Tbulk FROM DATA FILE
* WRITE Tsurface, Tbulk, Heat Flux, Nusselt, Rayleigh, Nusselt(Chur)*
* Tfilm, beta, density, viscosity, Cp, conductivity, latent heat,
* Prantl, surface tension
* *****
* OPEN (UNIT=1, FILE=' INPUT. DAT', STATUS=' OLD' )
* OPEN (UNIT=2, FILE=' OUTPUT. DAT', STATUS=' NEW' )
* OPEN (UNIT=3, FILE=' PROPE1. DAT', STATUS=' NEW' )
* OPEN (UNIT=4, FILE=' PROPE2. DAT', STATUS=' NEW' )
* OPEN (UNIT=5, FILE=' ROHSE. DAT', STATUS=' NEW' )
*
* DO 15 I = 1, N
*   READ (1, *) TS(I), HF(I), TB(I)
*   TF(I) = (TS(I) + TB(I)) / 2.
*   TF1(I) = TF(I) + 273.15
*   BETA(I) = 0.00261 / (1.740 - 0.00261 * TB(I))
*   PRINT*, 'BETA IS ', BETA(I)
*   DIA = 0.005 * 0.0254
*   G = 9.81
*   TSAT = 56.
*   WS(I) = TS(I) - TSAT
*   DENF(I) = (1.740 - 0.00261 * TB(I)) * 1000.
*
*   V(I) = (246 - 10.93 * TB(I) + 0.213 * TB(I) ** 2 - 19.3E-4 * TB(I) ** 3 +
+ 6.55E-6 * TB(I) ** 4) / 338.
*   DENV(I) = 1. / V(I)
*   KINV(I) = (0.54 - 0.0116 * TB(I) + 0.0002085 * TB(I) ** 2) * 1E-6
*   CP(I) = (0.241111 + 3.7037E-4 * TB(I)) * 4186.
*   K(I) = (-0.00115 * TF(I) + 0.6033) / 10.
*   HFG(I) = (8057 - 22.73 * TB(I)) * 10.79
*
*   ALF(I) = K(I) / (DENF(I) * CP(I))
*   PR(I) = KINV(I) / ALF(I)
*   SURT(I) = (-0.12 * TF(I) + 15) / 1000.
*   MU(I) = KINV(I) * DENV(I)
*
C *****
C Y(I) = (HF(I) / (MU(I) * HFG(I))) * SQRT(SURT(I) / (G * (DENF(I) - DENV(I))))
C X(I) = CP(I) * (TS(I) - TB(I)) / (HFG(I) * PR(I) ** 1.7)
C CSF(I) = X(I) / (Y(I) ** 0.333)
C *****
C CALCULATE RAYLEIGH and NUSSOLT NUMBERS
C *****
* RAYD(I) = G * BETA(I) * (TS(I) - TB(I)) * DIA ** 3 / (KINV(I) * ALF(I))
* RAYFB(I) = G * BETA(I) * HF(I) * DIA ** 4 / (K(I) * KINV(I) * ALF(I))
* NUSEX(I) = HF(I) * DIA / (K(I) * (TS(I) - TB(I)))
* NUSC(I) = (0.60 + (0.387 * RAYD(I) ** (1./6.) / ((1 + (0.559 / PR(I)) ** (
+ 9./16.)) ** (8./27.)))) ** 2
*
* WRITE (2, 20) TS(I), TB(I), HF(I), NUSEX(I), RAYD(I), NUSC(I)
* WRITE (3, 30) TF(I), BETA(I), DENF(I), DENV(I), KINV(I), CP(I)
* WRITE (4, 40) K(I), HFG(I), ALF(I), PR(I), SURT(I)
* WRITE (5, 50) Y(I), X(I), CSF(I)
20 FORMAT (1X, F8.2, 2X, F9.1, 2X, F12.2, 2X, F8.3, 2X, F12.7, 2X, F15.3 )
30 FORMAT (1X, F8.4, 2X, F9.4, 2X, F9.1, 2X, F8.4, 2X, E10.3, 2X, F15.3 )
40 FORMAT (1X, F8.4, 2X, F14.4, 2X, E10.3, 2X, F14.4, 2X, F9.5 )
50 FORMAT (1X, F8.4, 2X, F14.4, 2X, E10.3 )
15 CONTINUE

```

## LIST OF REFERENCES

3M Corp., *Flourinert Product Manual*, Commercial Chemicals Division: St. Paul, Minnesota, 1987.

Bar-Cohen, A., and T. Simon, "Wall Superheat Excursions in the Boiling Incipience of Dielectric Fluids," *Heat Transfer Engineering*, Vol. 9, no. 3., pp. 19-31.

Bar-Cohen, A., and T. Simon, *Experiments on Boiling Incipience with a Highly-Wetting Dielectric Fluid: Effects of Pressure, Subcooling, Dissolved Gas Content*.

Benedict, T., *An Advanced Study of Natural Convection Immersion Cooling of a 3x3 Array of Simulated Components in an Enclosure Filled with Dielectric Liquid*, Master's Thesis, Naval Postgraduate School: Monterey, California, June 1988.

Berenson, P.J., "Experiments on Pool-Boiling Heat Transfer," *International Journal of Heat Mass Transfer*, Vol. 5, pp. 985-999, 1962.

Bergles, A., N. Bakhru, and J. Shires, "Cooling of High Power Density Computer Components," Department of Mechanical Engineering Projects Laboratory Report, Massachusetts Institute of Technology, 1968.

Bergles, A. and Chyu, "Nucleate Boiling from Porous Metal Coatings," *Energy Conservation via Heat Transfer Enhancement*, Department of Energy Publication C00-4649-10, pp. 5-13, 1979.

Chowdhury, S.K.R., and R.H.S. Winterton, "Surface Effects in Pool Boiling," *International Journal of Heat Mass Transfer*, Vol. 28, pp. 1881-1889, 1985.

Churchill, S.W., and H.H.S. Chu, "Correlating Equations for Laminar and Turbulent Free Convection from a Horizontal Cylinder," *International Journal of Heat Mass Transfer*, Vol. 18, p. 1049, 1975.

Frost, W., and G.S. Dzakowic, "An Extension of the Method of Predicting Incipient Boiling on Commercially Finished Surfaces," ASME paper 67-HT-61, 1967.

Hazard, J., *Single Phase Liquid Immersion Cooling of Discrete Heat Sources on a Vertical Channel*, Master's Thesis, Naval Postgraduate School: Monterey, California, December 1986.

Incropera, F.P., and D.P. DeWitt, *Introduction to Heat Transfer*, (John Wiley & Sons, 1976).

Kaye, G.W.C. and T.H. Laby, *Tables of Physical and Chemical Constants and Some Mathematical Functions*, 14th ed., (London: Longman), p. 104.

Lee, T.Y., and T.W. Simon, "High-Heat-Flux Forced Convection Boiling from Small Region," *Heat Transfer in Electronics*, ASME HTD-Vol. 111, pp. 7-16, 1989.

Lepere, V., *Nucleate Pool Boiling of High Dielectric Fluids from Enhanced Surfaces*, Master's Thesis, Naval Postgraduate School: Monterey, California, December 1980.

McAdams, W.H., W.E. Kennel, C.S. Minden, Rudolf Carl, P.M. Picornell, and J.E. Dew, "Heat Transfer at High Rates to Water with Surface Boiling," *Industrial and Engineering Chemistry*, vol. 41, No. 9, 1949.

Mudawar, I., and D.E. Maddox, *Critical Heat Flux in Subcooled Flow Boiling of Fluorocarbon Liquid on a Simulated Electronic Chip in a Vertical Rectangular Channel*.

Nishikawa, K., and T. Ito, "Augmentation of Nucleate Boiling Heat Transfer by Prepared Surfaces," Japan-United States Heat Transfer Joint Seminar, Tokyo, Japan, 1980.

Okuyama, Kunito, and Yoshihiro Ida, *Transient Boiling Heat Transfer Characteristics of Nitrogen*.

Rohsenow, W.M., "Boiling," *Handbook of Heat Transfers*, W.M. Rohsenow and J.P. Hartnett, eds., (New York: McGraw Hill, 1973), chapter 13.

Tang, W., A. Bar-Cohen and T. Simon, *Thermal Transport Mechanisms in Nucleate Pool Boiling of Highly-Wetting Liquids*.

Torikai, K., H. Shimamune, and T. Fujishiro, "The Effects of Dissolved Gas Content upon Incipient Boiling Superheats," *Proceedings of the 4th International Heat Transfer Conference*, Vol. V., B2.11, 1970.

Yilmaz, S., J. Hwalek, and J. Westwater, "Pool Boiling Heat Transfer Performance for Commercial Enhanced Tube Surfaces," ASME Paper No. 80-HT-41, National Heat Transfer Conference, Orlando, Florida, 1980.

You, S.M., "Boiling Heat Transfer with Highly-Wetting Dielectric Fluids," Ph.D. Thesis, University of Minnesota, 1990.

You, S.M., T.W. Simon, A. Bar-Cohen, and W. Tang,  
"Experimental Investigation of Nucleate Boiling Incipience  
with a Highly Wetting Dielectric Fluid (R-113)," to appear in  
the *International Journal of Heat and Mass Trans.*



# INITIAL DISTRIBUTION LIST

	No. Copies
1. Defense Technical Information Center Cameron Station Alexandria, Virginia 22304-6145	2
2. Library, Code 52 Naval Postgraduate School Monterey, California 93940	2
3. Mechanical Engineering Curricular Office, Code ME Naval Postgraduate School Monterey, California 30340	1
4. Professor M.D. Kelleher, Code ME/Kk Naval Postgraduate School Monterey, California 93943-5000	2
5. Professor Y. Joshi, Code ME/Ji Naval Postgraduate School Monterey, California 93943-5000	1
6. Naval Weapons Supppport Center Code 6042 Crane, IN 47522	1
7. Dz K. Komutanligi Okullar ve Kurslar Dairesi Bakanliklar, Ankara, Turkey	1
8. Deniz Harp Okulu Kütüphanesi Tuzla, Istanbul, Turkey	1
9. Istanbul Teknik Üniversitesi Makine Fakültesi Kytyphanesi Istanbul, Turkey	1
10. LTJG Ali Sükrü Eren Harzem Sok 5/3, 80650 Çeliktepe, Istanbul, Turkey	2
11. LT R.A. Egger SMC #1039 Naval Postgraduate School Monterey, California 93943-5000	1